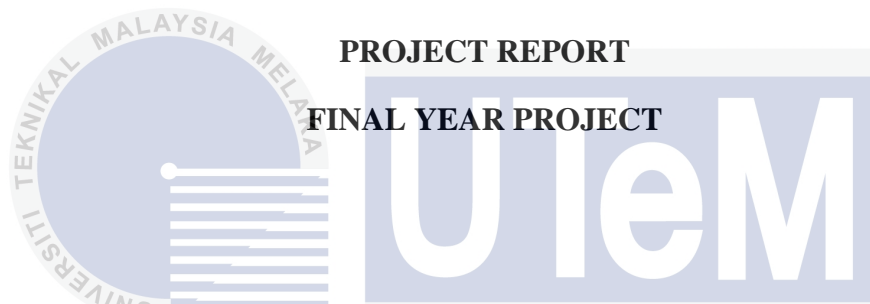




**FAKULTI KEJURUTERAAN ELETRIK (FKE)**

**UNIVERSITI TEKNIKAL MALAYSIA MELAKA**



**PROJECT REPORT**

**FINAL YEAR PROJECT**

**DESIGN AND DEVELOPMENT AN INSTRUMENT FOR ROAD WIDTH  
MEASUREMENT**

اونيورسي تيكنيكل مليسيا ملاك  
**UNIVERSITI TEKNIKAL MALAYSIA MELAKA**

**SAIFUL ANWAR BIN HASNAWI**

**BACHELOR OF MECHATRONIC ENGINEERING**

**JUNE 2014**

DESIGN AND DEVELOPMENT AN INSTRUMENT FOR ROAD WIDTH  
MEASUREMENT

SAIFUL ANWAR BIN HASNAWI



This is submitted in fulfillment of the requirement for the awards of the degree of

**Bachelor of Mechatronic Engineering**

Faculty of Electrical Engineering

UNIVERSITI TEKNIKAL MALAYSIA MELAKA (UTeM)

“I hereby declare that this report entitle “Design and Development An Instrument For Road Width Measurement” is the result of my own research except as cited in the references. The report has been not accepted for any degree and is not concurrently submitted in candidature of any other degree”

Signature	:	
Name	:	SAIFUL ANWAR BIN HASNAWI
Matrix Number	:	B011010329
Date	:	اونيورسيتي تيكنيكل مليسيا ملاك

---

UNIVERSITI TEKNIKAL MALAYSIA MELAKA

“I declare that I have read through this report entitle “Design and Development An Instrument For Road Width Measurement” and found that it has comply the partial fulfillment for awarding the degree of Bachelor of Mechatronic Engineering”



## ACKNOWLEDGMENT

All praises to ALLAH S.W.T. the Almighty God that has given us the strength, the ideas and many other things upon this final year project. A very greet to our Prophet Muhammad S.A.W., his family and friends. Your blessing gives me an opportunity and some ideas to complete my final year project.

I would like to convey my thankfulness to my supervisor, Nur Latif Azyze Bin Mohd Shaari Azyze for guidance throughout the progress of this project, for his nascent ideas, valuable guidance and continuous encouragement. This project report would not be possible completed without his guidance. I appreciate his countless hours spent in sharing his understanding, knowledge and experience throughout in this project.

At the end, I would like to express my great appreciation to my beloved parents and family who have been supporting me during my study in UTeM. Special thank also go to my friends especially my housemates for their co-operation and supports during this study. Lastly, thanks to everyone who has contributed in completing this project.

## ABSTRACT

The present studies about road and road-edge detection are mainly based on laser sensor, LIDAR sensor, laser radar, frequency modulated continuous wave (FMCW) radar and machine vision. In this project, an instrument was developed for road and road-edge detection to measure road width. It was also may be used on the road line painting mobile robot. The device is based on the ultrasonic sensor. Nowadays, the process of road line painting was done manually by human. It takes many time, money and manpower. Workers also were at risk to have an accident during painting the road lines and it may be fatal. The objectives for this project are to design an instrument to measure road width and to analyse the accuracy and the reliability of the sensor for road width measurement. The project was used an ultrasonic sensor as a road region detection. The rotating of ultrasonic sensor have ranging the road region to detect the road edge. The ultrasound wave transmit to the road region reflected to the receiver. The time of flight is determined as well as the distance between the sensor and the road surface. The road surface profile was plotted and display on the computer. Several experiments were done by the instrument and the results showed the proposed method on accuracy and reliability.

## ABSTRAK

Kajian semasa dalam pengesanan jalan raya dan tebing jalan adalah berdasarkan sensor laser, sensor LIDAR, laser radar, kekerapan gelombang termodulat berterusan (FMCW) radar dan penglihatan mesin. Dalam projek ini, instrument telah dibangunkan untuk pengesanan jalan raya dan tebing jalan untuk mengukur lebar jalan. Ia juga boleh digunakan pada robot mudah alih untuk mengecat garisan jalan. Peranti ini berdasarkan sensor ultrasonik. Pada masa kini, proses mengecat garis jalan dilakukan secara manual oleh manusia. Proses ini memerlukan banyak masa, wang dan tenaga manusia. Pekerja juga berisiko untuk mendapat kemalangan semasa mengecat garisan jalan dan ia boleh membawa maut. Dalam usaha untuk mengurangkannya, instrumen ini telah dibangunkan. Objektif projek ini adalah untuk merekabentuk sebuah instrumen untuk mengukur lebar jalan dan menganalisis ketepatan dan kebolehpercayaan sensor untuk ukuran lebar jalan raya. Projek ini menggunakan sensor ultrasonik sebagai pengesan kawasan jalan raya. Sensor ultrasonik ini yang berputar mengimbas kawasan jalan raya untuk mengesan tebing jalan raya. Gelombang ultrasonik dipancarkan ke kawasan jalan dan gelombang yang terpantul ditujukan kepada penerima. Masa penerbangan data ditentukan serta jarak antara sensor dan permukaan jalan. Profil permukaan jalan dibina dan dipaparkan pada komputer. Beberapa eksperimen dijalankan dan keputusan yang terhasil menunjukkan kaedah yang dicadangkan adalah tepat dan boleh dipercayai.

## TABLE OF CONTENTS

CHAPTER	TITLE	PAGE
	<b>ACKNOWLEDGMENT</b>	<b>v</b>
	<b>ABSTRACT</b>	<b>vi</b>
	<b>TABLE OF CONTENTS</b>	<b>viii</b>
	<b>LIST OF TABLES</b>	<b>xi</b>
	<b>LIST OF FIGURES</b>	<b>xiii</b>
<b>1</b>	<b>INTRODUCTION</b>	<b>1</b>
	1.1 Introduction	1
	1.2 Project Background	1
	1.3 Motivation	2
	1.4 Problem Statement	3
	1.5 Objective	4
	1.6 Scope and Limitation	4
<b>2</b>	<b>LITERATURE REVIEW</b>	<b>5</b>
	2.1 Definition of Sensor	5
	2.2 Classification of Sensor	6
	2.3 Characteristic of Sensor	6
	2.4 Ultrasonic Sensor	7
	2.5 Radar	8
	2.5.1 Basic Principle	8
	2.5.2 Principle of Measurement	8
	2.5.3 Classification of Radar	10
	2.5.4 Antenna	11
	2.2 Related Previous Works	11
	2.2.1 Road Boundary Recognition Using Laser Sensor	11



2.2.2 Road and Road Edge Detection Using LIDAR Sensor	17
2.2.3 Structural Road Detection Based on a 2D Laser Radar	23
2.2.4 Road Edge Detection System using FMCW Radar	28
2.2.5 Road Boundary Detection Based on Vision	34
2.3 Summary of Review	37
<b>3 METHODOLOGY</b>	<b>38</b>
3.1 Introduction	38
3.2 Process Flow Chart	39
3.2 System Overview	41
3.3 Hardware Section	41
3.4 Sensor	42
3.5 Motor	44
3.6 Microcontroller	45
3.7 Hardware of the Ultrasonic Sensor	46
3.8 Software	46
3.9 Experiment and Data Collection	47
3.9.1 Rotation Speed for Servo Motor Experiment	48
3.9.2 Accuracy of Instrument Experiment	50
3.9.3 Reliability of Instrument Experiment	52
3.10 Summary	54
<b>4 RESULT AND ANALYSIS</b>	<b>56</b>
4.1 Sensor Design	56
4.2 Data Collection	59
4.2.1 Rotation Speed of Servo Motor Testing	59
4.2.2 Accuracy Testing	60
4.2.3 Reliability Testing	65
4.3 Analysis and Discussion	70
4.3.1 Rotation Speed of Servo Motor Testing	70
4.3.2 Accuracy Testing	72
4.3.3 Reliability Testing	77

<b>5</b>	<b>CONCLUSION AND RECOMMENDATIONS</b>	<b>84</b>
	5.1 Conclusion	84
	5.2 Recommendation	85
	<b>REFERENCES</b>	<b>86</b>
	<b>APPENDIX</b>	<b>88</b>



## LIST OF TABLES

TABLE	TITLE	PAGE
2.1	Result for simulation $S1$	27
2.1	Result in simulation $S2$	27
4.1	Average distance between sensor and road model surface for every time delay function	59
4.2	Distance between sensor and road surface vs Angle of rotation	61
4.3	Distance between sensor and road surface vs Angle of rotation	63
4.4	Distance between sensor and road surface for 30 trials	66
4.5	Distance between sensor and road surface for 30 trials	68
4.6	Initial angle of road region, $\theta_i$ and final angle of road region, $\theta_f$ for every time delay function	70
4.7	Percentage of error and Percentage of accuracy for every time delay function	71
4.8	Initial angle of road region, $\theta_i$ and final angle of road region, $\theta_f$ for 10 trials	72
4.9	Initial angle of road region, $\theta_i$ and final angle of road region, $\theta_f$ for 10 trials	73
4.10	Percentage of error and Percentage of accuracy for 10 trials	74
4.11	Percentage of error and Percentage of accuracy for 10 trials	75
4.12	Initial angle of road region, $\theta_i$ and final angle of road region, $\theta_f$ for 30 trials	77
4.13	Initial angle of road region, $\theta_i$ and final angle of road region, $\theta_f$ for 30 trials	78
4.14	Percentage of error, Percentage of accuracy and Precision value for 30 trials	80

4.15	Percentage of error, Percentage of accuracy and Precision value for 30 trials	82
------	---	----



## LIST OF FIGURES

FIGURE	TITLE	PAGE
2.1	Classification of radar type [6]	10
2.2	Working principle of the laser sensor[8]	12
2.3	Banner LT3 laser sensor[8]	12
2.4	Collecting road boundary points[8]	13
2.5	Scanning of road boundary[8]	13
2.6	Coordinate of road boundary points in the moving coordinate system[8]	15
2.7	Sketch of collected data[8]	16
2.8	Sketch of fitted road boundary[8]	16
2.9	LMS-200 SICK sensor[9]	18
2.10	Flowchart of road/road edge detection algorithm[9]	18
2.11	Selection of road segment region candidate[9]	19
2.12	Calculation of weight standard deviation[9]	19
2.13	Result of region classification[9]	20
2.14	Result of road curb detection[9]	21
2.15	Single scan detection result[9]	21
2.16	Multiple scan detection result[9]	22
2.17	An unsmoothed road in radar map[11]	23
2.18	An unclear edge on road in radar map[11]	24
2.19	Vehicle is not parallel with road in radar map[11]	24
2.20	Road points covered by the rectangle[11]	24
2.21	Laser radar scanning principle[11]	25
2.22	Rectangle (green colour) with different slopes cover the road points (magenta colour)[11]	26
2.23	Block Diagram of FMCW Radar[12]	28

2.24	Scanning technique by radar system[12]	29
2.25	Steep road edge road edge[12]	30
2.26	Altitude based profile for steep road edge[12]	30
2.27	Negative slope road edge[12]	31
2.28	Altitude based profile for negative slope road edge[12]	31
2.29	Asphalt road shoulder[12]	32
2.30	Altitude based profile for asphalt road shoulder[12]	32
2.31	Flowchart of road detection[13]	34
2.32	The original image of road[13]	36
2.33	The final image of road[13]	36
3.1	PSM flowchart	39
3.2	Methodology flowchart	40
3.3	Upper part of instrument	42
3.4	SN LV-MaxSonar-EZ1 ultrasonic sensor dimensions	43
3.5	Beam characteristic for SN LV-MaxSonar-EZ1 ultrasonic sensor	43
3.6	Pan-tilt servo motor	44
3.7	Pulse Width Modulation	45
3.8	Arduino UNO	46
3.9	Experiment setup on the road model	50
3.10	Experiment setup on the road with 1 lane	52
3.11	Experiment setup on the road had road curb	54
4.1	Isometric view of sensor	57
4.2	Front view of sensor	58
4.3	Top view of sensor	58
4.4	Graph of road model profile for 50 ms, 40 ms, 30 ms, 20 ms, 10 ms time delay functions	60
4.5	Graph of road profile for average 10 times of data	62
4.6	Graph of road profile for average 10 times of data	65
4.7	Graph of Percentage accuracy vs No. of Trials (road with 1 lane)	74
4.8	Graph of Percentage accuracy vs No. of Trials (road had road curb)	76
4.9	Graph of Percentage accuracy vs No. of Trials (road with 1 lane)	81

4.10	Graph of Precision value vs No. of Trials (road with 1 lane)	81
4.11	Graph of Percentage accuracy vs No. of Trials (road had road curb)	83
4.12	Graph of Precision value vs No. of Trials (road had road curb)	83



## CHAPTER 1

### INTRODUCTION

#### 1.1 Introduction

In this chapter, the purpose of this project was described generally. This chapter started with problem related with current issues then implemented into problem statement. After that, the objectives of the project are created to solve the problem statement. The project scope also stated to cover the limitations for this project.

#### 1.2 Project Background

An instrument is a device used to determine the value of the quantity under measurement meanwhile, a sensor is a device to detect and respond to electrical or optical signals or stimulus. Sensors act as a converter of physical parameter or stimulus such as temperature, light, distance and humidity into an electrical signal that can be measured and read by an instrument. In various system, a transducer may use as an actuators. These actuators converts electrical signal into generally non-electrical energy. As an example, an electric motor is an actuator. The motor converts electric energy into mechanical energy.

Road edge detection is currently study by many researchers for applications in automated guided vehicles and mainly done through the optical images using machine vision. The studies is also an essential component in autonomous vehicle for navigation. The navigation is focused on the monitoring and controlling the movement autonomous vehicle



like mobile robot, therefore the research and development of mobile robots have a great future in multi-tasking application. The robot is mainly use in the industry sector to make the task going easily and smoothly. The usage of robot also can save time and cost, hence it may helping to increase the working productivity and efficiency. Mobile robot can be found in military, industry and security services but it is no use the robot for road line painting task. Recently, this task is done manually by human. The worker pushing the road line painting machine along the road to paint the road line. Another example, the worker drive the road line painting machine to mark the road line. By using this robot, the task to paint the road line easier and reduces time, cost and also the human power.

Therefore, the instrument that designed in this project is built, to detect road edge and calculate the road width. The sensor that used in this project is ultrasonic sensor. This sensor scans the road  $180^\circ$  to find the road edge and road region. Ultrasound wave transmit the signal to the road regions and received it back after the signal is reflected by road surface. This sensor is rotated with the help of servo motor. The signal is processed and the road surface profile is displayed with the road width measurement.

### 1.3 Motivation

Nowadays, the road construction plays an important role in nation development to provide better infrastructures and facilities. Good public transportation service also require better road facility. Better road construction built also help human for travelling and it can reduce the travelling time when we go to other places. At the same time, road line construction is also happen. Road line guide the vehicle's user during driving on the road. Traditionally, the process of road line painting is done manually by human. Firstly, the workers need to measure the road width. Next, the worker make a guidance along the road edge with a nylon thread. Then, the workers need to walk along the road when pushing the road line painting machine. Based on an article from [1], the workers may to involve in an accident while they paints the road line. They also works in a hot weather. Besides, the process to paint the road line by human is taking a lot of time.

This study is about to design and develop an instrument for road width measurement. This device is also can be attached on the road line painting mobile robot. This device is

provided the measurement of road width to use in road line painting process. It can save time, money and manpower. At the end, this project make the road line painting process easier.

#### 1.4 Problem Statement

Road line painting is mainly important in the construction of the road. This line divide roads into several lanes and make sure vehicle's user drive in the lane. The road line also provide guidance to motorist when they ride at night condition. This line also increase the visibility of road at night and in bad weather. In the real world, road line painting job still be done manually by human. Workers are potential to have an accident while painting the road lines and can be fatal. The road line painting process can be done quickly by using the mobile robot. The mobile robot can save human life and time.

This project is to design and develop an instrument for road width measurement. The output from the device can be used in road line painting process. The road profile is plotted and determined the road edge from that profile. The calculation is done to obtain the road width. This sensor can be used on the robot. This project also introduces the new way for road line painting in Malaysia.

## 1.5 Objective

The main objectives for this project are:

- i. To design and develop an instrument to measure road width.
- ii. To analyse the accuracy and the reliability of the instrument for measuring road width.

## 1.6 Scope and Limitation

The scopes of work for this project are developing an instrument to measure road width by using road edge detection method. This is not include the obstacles like walls, trees and road dividers for measuring the road width. The road surface is used in the experiment must flat and clear from any obstacles. The input (ultrasonic sensor) and produce the output to control the motor and signal processing. The instrument also need to simulate and demonstrate the road surface profile as an output in the host computer.

## CHAPTER 2

### LITERATURE REVIEW

The general information of the sensor for road area detection was discussed in this chapter. The main purpose of the study is related to the type of sensor use and the selection of method for road edge detection. Other than that, the limitations of these methods were included in this study. The previous research information, methodologies and design will be used for references and guidelines in this project. The facts and information were collected from reliable source and elaborated based on the understanding of the review.

#### 2.1 Definition of Sensor\*

A sensor is a device to detect and respond to electrical or optical signals or stimulus. Sensors act as a converter of physical parameter or stimulus such as temperature, light, distance and humidity into an electrical signal which can be measured and read by an observer or by an instrument. In various system, transducer may use as actuators. The actuator converts electrical signal into generally nonelectrical energy. As an example, an electric motor is an actuator. The motor converts electric energy into mechanical energy [2].

## 2.2 Classification of Sensor

Sensor can be classified into two types, active and passive. A passive sensor is directly generates an electrical signal in response to an external stimulus and does not need any additional energy sources [7]. Besides, the input energy from stimulus is changed by the sensor into the output signal. A thermocouple, a photodiode and a piezoelectric sensor are the examples of passive sensor. Sensors that require external power for their operation is called an active sensor. The external power also called as an excitation signal. The output signal is produced from the sensor by modified the excitation signal [7]. The active sensor may call as parametric because of their properties change in response to an external effect and afterwards these properties converted into electric signals. The parameter of sensor is modulating the excitation signal and the modulation carries information of measured data. A resistive strain gauge is an example of active sensor which is the electrical resistance relates to a strain. The electric current must be applied to it from an external power source for measuring the resistance of a sensor [2] [3].

## 2.3 Characteristic of Sensor

The characteristic of sensor used to know their performance in data measurement. One of the sensor's properties is sensitivity. Sensitivity is defined as the ratio of the change in output of the sensor to a change in input parameter being measured. For examples, a thermometer with mercury inside it will expand or contract 1cm for every 1°C of temperature changes, it shows the sensitivity of thermometer is 1cm/°C. Another of characteristic of sensor is resolution. High resolution sensor is able to detect the smallest change in input parameter. Repeatability is the ability of a sensor to detect the same object at the same distance time after time. The sensor must able to collect the same data as the test is performed repeatedly. The difference between the operator (switch on) and release (switch off) points in proximity sensor when the target is moving away from the sensor face is called hysteresis. Sensors also have specified range to operate [2] [3].

## 2.4 Ultrasonic Sensor

Ultrasonic sensor is one of the active sensor. It also known as transceivers as they both send and received signal. It also act as the transducer because it generate sound from electrical energy and transform into electrical energy from sound. The working principle of this sensor are similar to radar and sonar where the detection of target by using the echo from sound waves. Ultrasonic sound waves are sound waves that are above the range of human hearing and, thus, have a frequency above about 20,000 hertz. It use high frequency sound waves to detect the presence of an object or surface with the presence of interruption of the sound beam. Distance between the sensor and the object can be determine by calculating the time interval between transmitting the signal and receiving the echo [2] [3].

$$L = \frac{vt}{2} \quad (1)$$

(1) is the equation of time of flight, where  $L$  the distance between sensor and target is,  $v$  is the speed of sound wave and  $t$  is the time travel of sound wave to target and back to the sensor [2].

The advantages of ultrasonic sensor are not affected by dust, dirt or high moisture environment, can measure and detects distances to moving objects. It also can detect small object on long operating distances [4]. In paper [5], the ultrasonic sensor is used to develop a map building which is apply the time of flight information. The ultrasonic sensor is rotated at small step of angle and time interval was taken.

Target Angle is refer to the tilt response limitation of sensor. Target angel also indicates the amount of acceptable tilt for a given sensor. Beam Spread defines as the area in which a round wand will be sensed if passed through the target area. It also provide the information about the maximum spreading of the ultrasonic sound as it goes toward the target [2].

## 2.5 Radar

### 2.5.1 Basic Principle

An object detection system which uses microwaves to determine the range, altitude, direction, or speed of objects is a radar. The basic principle of radar is the radar antenna radiate the microwave signal to the target then the signal is reflected back and picked up by the receiver. The reflected signal also called as echo. Transmitter generated the radar signal and received back by the sensitive receiver. The diffuse reflection was produced by the object or target and it is reflected in numbers of direction. The reflection in the opposite direction to the incident rays is called backscatter. The radar system consist of transmitter, receiver, duplexer, radar antenna and indicator. The transmitter works to generate the short duration radio frequency pulse of energy into the space by the antenna. Amplify and demodulate the received signal and provides the video signal as the output is called the receiver. The duplexer act as a switch, switching the antenna between the transmitter and the receiver so the antenna only used once at a time. It is to avoid the high power pulse from the transmitter to enter the receiver. Transferring the transmitter signal into the space is required by the antenna. It also need a distribution pattern and efficiency. Indicator present a continuous and graphical display of the relative position of the target to the observer or operator [6] [7].

UNIVERSITI TEKNIKAL MALAYSIA MELAKA

### 2.5.2 Principle of Measurements

Time delay ranging is the fundamental parameter that measured in radar system. It is involve of round trip time of the pulse and the velocity of light. There are two types of radar, bistatic radar and monostatic radar. For bistatic radar, the transmitter and the receiver are located at different locations and for monostatic radar, both of transmitter and receiver are located at same place. Assume the  $R_t$  is distance of target from transmitter,  $R_r$  is the distance of target from receiver,  $c$  is speed of light and  $T_f$  is round trip time. The (2) and (3) is the equation of time delay ranging for bistatic and monostatic radar respectively [7].

$$\text{Bistatic radar, } R_t + R_r = cT_f \quad (2)$$

$$\text{Monostatic radar, } R = cT_f/2 \quad (3)$$

Pulse repetition frequency, PRF is a reciprocal pulse repetition time, PRT which is the time of the beginning of one pulse to the start of next pulse. Radar send pulse during a time and wait the echo (reflected signal) to come back and then start again send the pulse, that period of time is called pulse repetition time [7].

Range ambiguity is an error of echo recognition by the radar. Radar transmit the first pulse and its echo is received after the transmission of pulse but the radar treat it as the second echo from the second pulse. Assume pulse width is  $\tau$ . (4) is the equation of range ambiguity[7].

$$\text{Range ambiguity} = \frac{[(PRT - \tau) * c]}{2} \quad (4)$$

Minimum detectable range,  $R_{min}$  is a blind range where the targets in close vicinity are not detected.  $t_{rec}$  is recovery time of a duplexer. (5) is the equation of minimum detectable range [7].

$$R_{min} = \frac{[(\tau + t_{rec}) * c]}{2} \quad (5)$$

Theoretical maximum range is expressed by the relationship between various parameter to determine the maximum radar range [7].

$$Pr = Pt \left[ \frac{G^2 * \lambda^2 * \sigma t}{(4\pi)^3 * R^4 * L} \right] \quad (6)$$

The equation (6) is for power returned to the target. Where,  $Pr$  is power returned to the target,  $Pt$  is transmitted power,  $G$  is the antenna gain,  $\lambda$  is the signal wavelength,  $\sigma t$  is the radar cross section,  $R$  is the slant range and  $L$  is the loss factor. (7) is the equation for maximum range detectable [7].



$$R_{max} = \sqrt[4]{\frac{Pt * G^2 * \lambda^2 * \sigma t}{(4\pi)^3 * Pr_{min} * L}} \quad (7)$$

### 2.5.3 Classification of radar

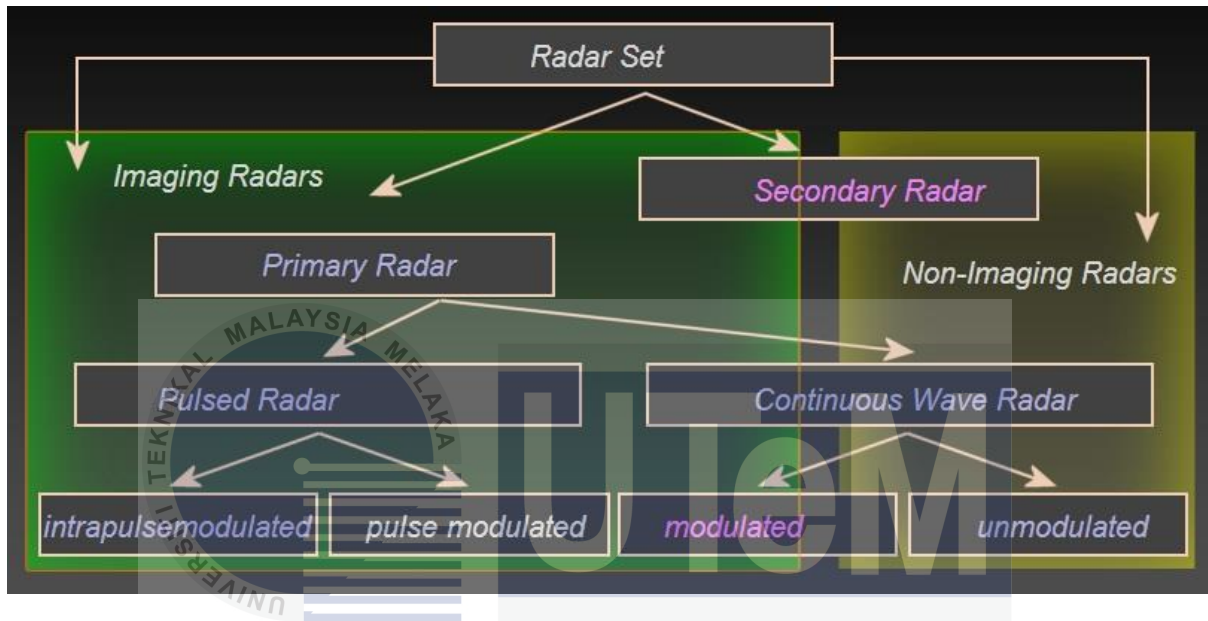


Figure 2.1 Classification of radar type [6]

Primary radar consist of pulsed radar and continuous wave radar. Pulsed radar transmit a short RF-signal of high power and take a longer break to receive an echo before a new transmitted signal is strike out. It can determine direction, distance and altitude of the target from measured antenna position and propagation time of the pulse signal. Pulsed radar divided into two type, intra-pulse modulated and pulse modulated. Intra-pulse modulated transmit weak pulse in the longer pulse width. Hence, pulse modulated transmit a very short pulse with high power to obtain a good range resolution [6].

Besides, the continuous wave radar transmit a high-frequency signal continuously and the echo is received, processed to prevent a direct connection of the transmitted energy into the receiver. Modulated continuous radar transmit the signal with constant amplitude but modulated in the frequency. The principle of the propagation time is used in this type. Moreover, the measurement result is continuously obtained. In contrast, the unmodulated continuous wave radar transmit signal with constant amplitude and frequency. This type is

specialised in speed measuring and one of the application is used as the speed gauges of the police [6].

#### **2.5.4 Antenna**

The function of the antenna is to transmit the microwave signal into the space and also to receive back the signal when it's reflected by the target or object. Antenna gain is the important characteristic of the antenna. The gain is the ratio between the amount energy propagated in a direction compared to the energy that would be propagated with no direction. The antenna used for transmit and receive the signal will have same gain in both process [6].

### **2.6 Related Previous Works**

Robot navigation plays an important role for the mobile robot. It means the robot's ability to determine its own position from in its frame of references and then plan a path towards the target. Road detection is a key task in developing robot navigation for mobile robot. Robot moves by followed the detection of road edge, curbs or road lanes. Several of methods for road detection has been used by the researcher in their design for mobile robot such as machine vision, frequency modulated continuous wave (FMCW) radar, laser scanner and laser range finder.

#### **2.6.1 Road Boundary Recognition Using Laser Sensor**

In paper [8], a method has been introduced by applying laser sensor to obtain road boundary points to solve road detection problems. The paper also introduces an algorithm for road boundary recognition including a way of extraction and coordinate calculation. Banner LT3 laser sensor is used on the mobile robot to recognize road boundary in this research. The working principle of laser sensor is laser pulse ranging, also known as Time of Flight (TOF). This principle obtains the distance value by transmitting light pulse to the

object and measure the round trip time. The working principle of laser sensor is shown in Fig 2.2 [8].

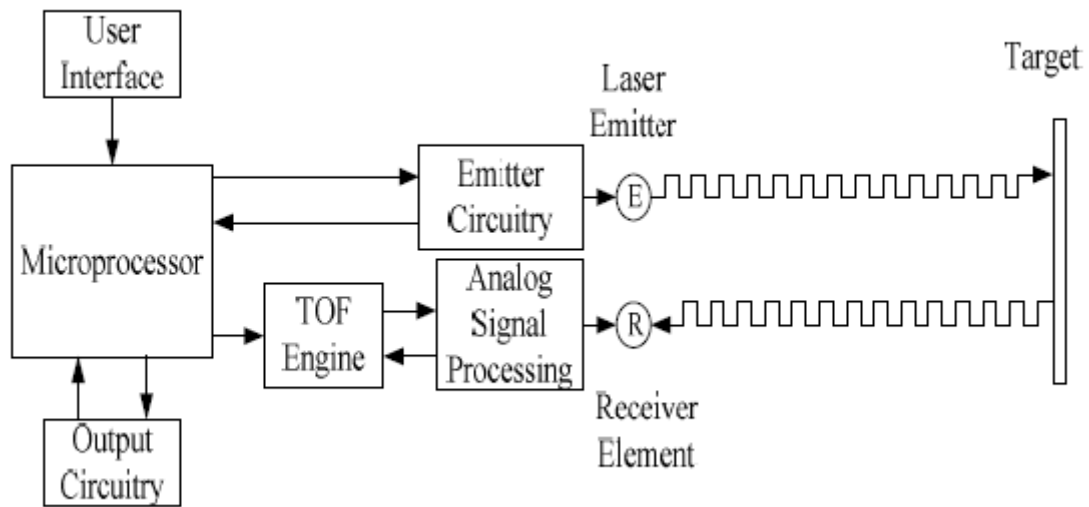


Figure 2.2 Working principle of the laser sensor[8]

The formula for calculation for this laser sensor can expressed as (8) [8].

$$D = V \cdot \frac{t}{2} \quad (8)$$

Where  $D$  the distance from the laser sensor to the object is,  $V$  is the velocity of light and  $t$  is the round trip time of the laser [8].



Figure 2.3 Banner LT3 laser sensor[8]

An algorithm is a specific method to solve problem using mathematical approach has been used for road boundary recognition in this paper. Position of mobile robot obtained by using absolute coordinate marked as  $(X_m, Y_m)$ . In Fig.3 shows how the road boundary points

is collected. The mobile robot represented by small triangle, zigzag stippling line shows the track was scanned and the mobile robot's motion track represents by the stippling line along  $Y'$  direction [8].

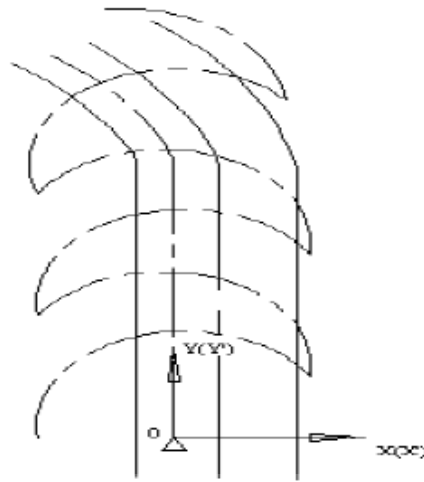


Figure 2.4 Collecting road boundary points[8]

The laser sensor equipped on the mobile robot scans the road  $180^\circ$  repeatedly when the robot moving forward along the road with  $Y'$  direction. Road boundary will reflect the track of laser points when the LT3 scans the road, the dashes lines with arrow are laser beams and points  $t_1, t_2, \dots, t_6$  are position points shows different distance values are reflected.  $t_4, t_5, t_6$  are the road boundary points with the smallest distance values[8].

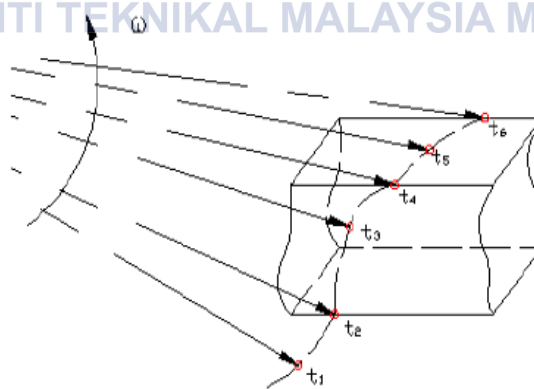


Figure 2.5 Scanning of road boundary[8]

To calculate the absolute coordinates of the road boundary points, the author was introduced these equations, (9) for x-coordinate of road boundary point and (10) is for y-coordinate of road boundary point [8].

$$X'_i = \pm d \quad (9)$$

$$Y'_i = \sqrt{(D \cdot \cos \emptyset)^2 - d^2} \quad (10)$$

Where  $(X'_i, Y'_i)$  is the coordinate of the road boundary points collected in moving coordinate system.  $D$  is the distance from point  $M$  to LT3 laser sensor.  $\emptyset$  is the declination angle of the LT3 laser sensor. The constant value,  $d$  is the distance of  $O'N$ .  $O'N$  represents the vertical distance from the robot's centre to the road boundary and point  $N$  is the perpendicular foot [8].

Then, the relationship between moving coordinate system and absolute one, the absolute coordinate of the road boundary points collected by the laser sensor can be expressed as (11) for x-coordinate point of absolute coordinate and (12) for y-coordinate point of absolute point [8].

$$X_{ci} = X_{mi} + X'_i \quad (11)$$

$$Y_{ci} = Y_{mi} + Y'_i \quad (12)$$

Where  $(X_{ci}, Y_{ci})$  is the absolute coordinate of the road boundary points collected at time  $i$ , while  $(X_{mi}, Y_{mi})$  is the absolute coordinate of the mobile robot at time  $i$  and  $(X'_i, Y'_i)$  is the coordinate of the road boundary points collected in moving coordinate system [8].

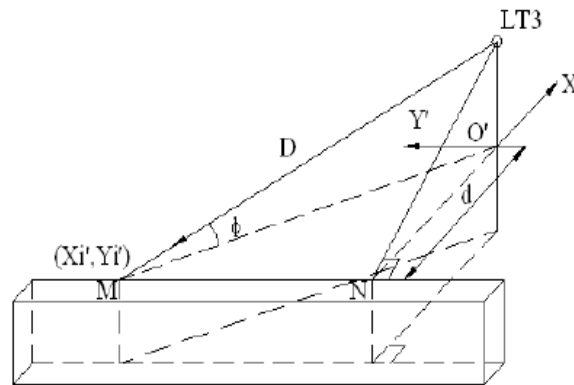


Figure 2.6 Coordinate of road boundary points in the moving coordinate system[8]

In paper [8], the experiment of road boundary was setup on flat road and the parameters are as follows [8]:

1. The height from the LT3 lasing point to the ground is 0.5m.
2. The LT3 laser sensor scans the road  $180^\circ$  repeatedly at uniform speed of 181 frames/s.
3. The speed of mobile robot is 0.5m/s and move in forward direction.
4. The width of road surface is 3m.

The result of this experiment is shown in Fig. 6 below.

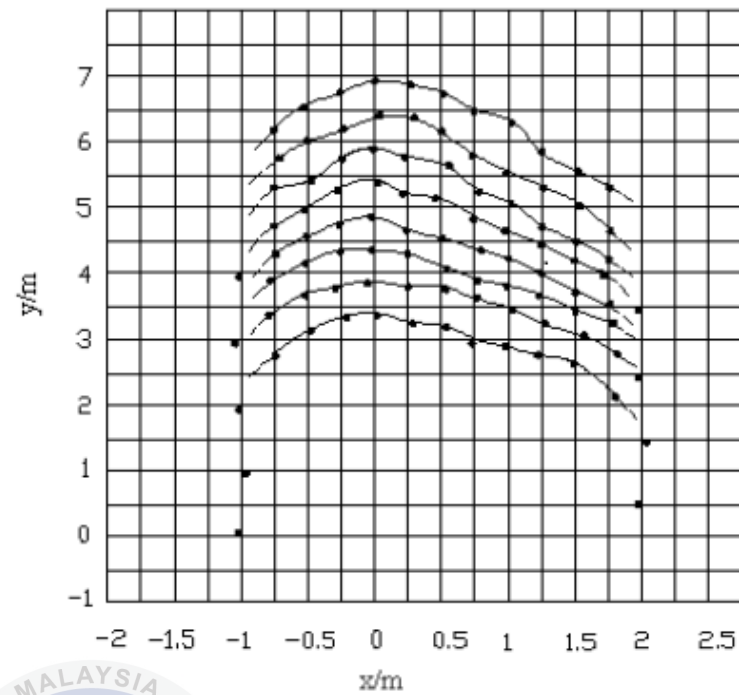


Figure 2.7 Sketch of collected data[8]

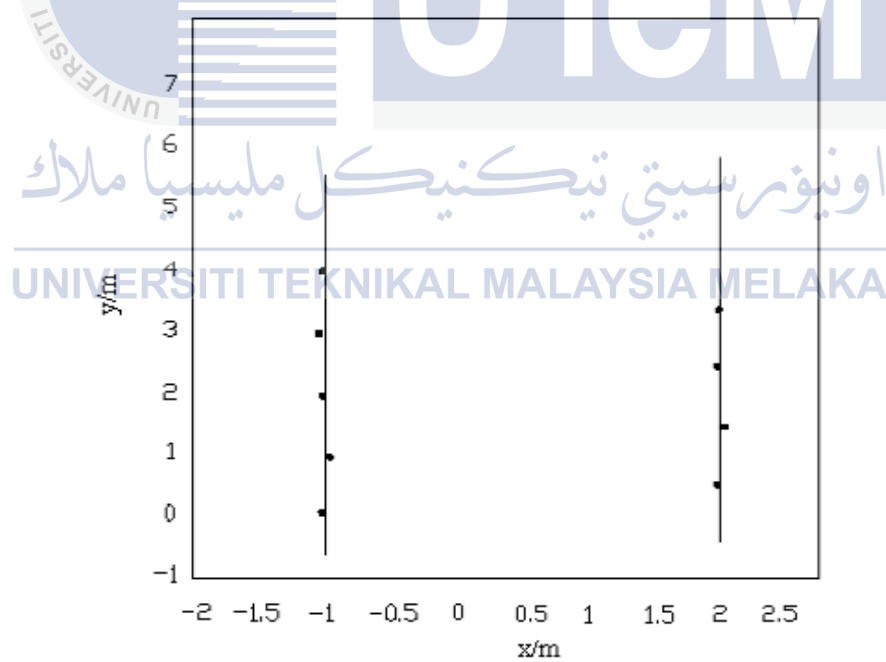


Figure 2.8 Sketch of fitted road boundary[8]

### 2.6.2 Road and Road Edge Detection Using LIDAR Sensor

Another method was proposed in paper [9] based on Light Detection and Ranging (LIDAR) sensor to identify road regions and road edges. LIDAR sensor can measure distance by lighting up a target with a laser and analyse the reflected light. This sensor using same working principle as laser sensor since this sensor using laser light [8]. This sensor measure the amount of time for each pulse of laser light to bounce back using this formula (13) [9].

$$D = V \cdot t / 2 \quad (13)$$

Where  $D$  the distance from the laser sensor to the object is,  $V$  is the velocity of light and  $t$  is the round trip time of the laser [9].

In addition, LIDAR sensor can measure the distance between the target and itself with high accuracy. In general, there are two types of LIDAR detection methods. Coherent detection and incoherent detection also known as direct energy detection. Coherent detection method usually use for Doppler or phase sensitive measurement. In that system, there use Optical heterodyne detection which is more sensitive than direct detection. It operates at much low power but has more complex transceiver requirement compared to incoherent detection method, which uses amplitude measurement. There are two main pulse models using in both types of LIDAR detection methods, micropulse and high energy system. Micropulse used more powerful computers and larger computational efficiency. This laser is lower powered and used safely. High energy system commonly used for atmospheric research and regularly use to measure atmospheric parameters like temperature, pressure, humidity and density of clouds. There are four main components in LIDAR sensor which is laser, scanner and optics, photodetector and electronics receiver and navigation and positioning system [9] [10].





Figure 2.9 LMS-200 SICK sensor[9]

The author used the LMS-200 SICK sensor to scan road boundary with two-dimensional point array covering 90 degree field of view with half degree resolution at a 75Hz scan rate. Assume the lowest smooth surface is the road and curbs are the road edge. The road edge algorithm used to analyse range data to detect road edge detection. The author also proposed a cascade processing method to detect road and road edge. There are five step in that process as shown in Fig. 8 [9].

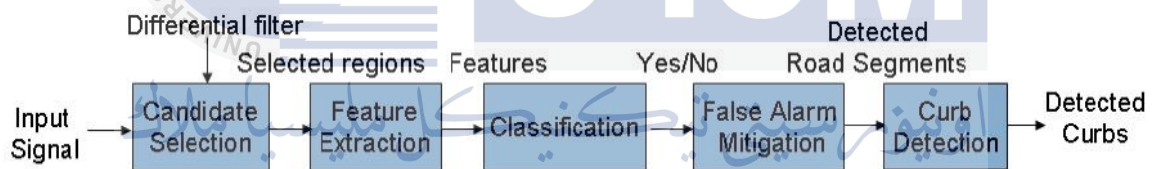


Figure 2.10 Flowchart of road/road edge detection algorithm[9]

In candidate selection process, the input signal is convolved with a Gaussian differential filter to identify local maximum points and local minimum points in the input signal. The regions between two local points selected to extract features for road segment classifications [9].

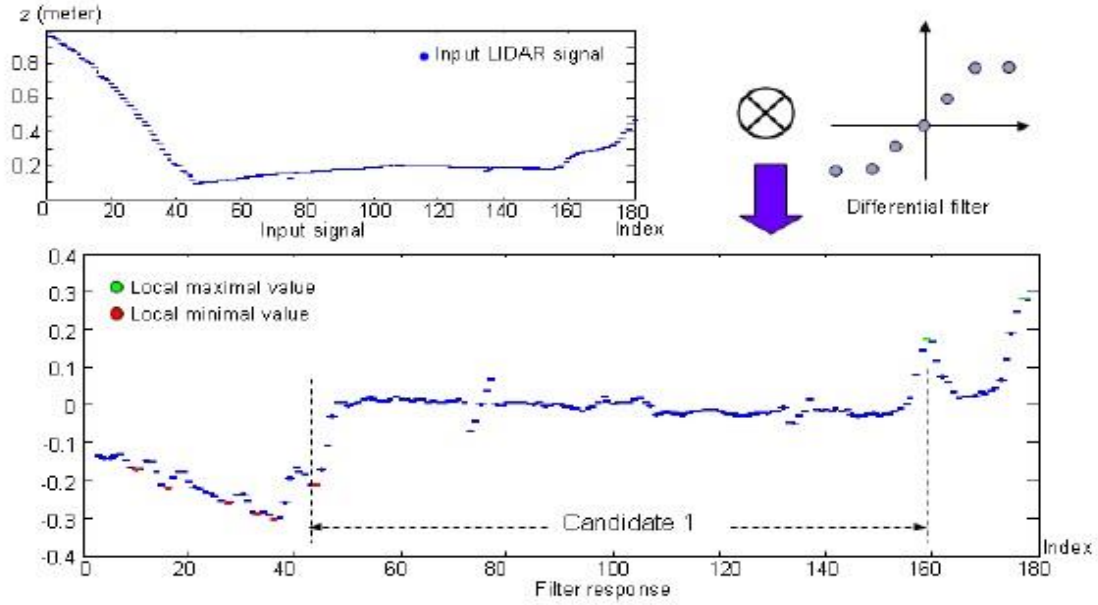


Figure 2.11 Selection of road segment region candidate[9]

Feature extraction process is to calculate the weight standard deviation  $\sigma_z$  of elevation  $z$  in the candidate road segment region using this equation. From the calculation, it is biased toward the centre region. (14) is the equation for weight standard deviation [9].

$$w(i) = \begin{cases} a(i), & a(i) \leq 1 \\ 1, & \text{otherwise} \end{cases}, a(i) = 2 \sin\left(i \cdot \frac{\pi}{(N-1)}\right), \quad i = 0, 1, 2, \dots, N-1 \quad (14)$$

Where  $N$  is the total number of points in the candidate region [9].

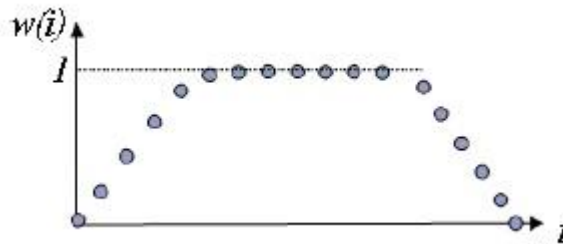


Figure 2.12 Calculation of weight standard deviation[2]

The classification process is needed to determine either the candidate region is a road segment to obtain the balance between the weighted standard deviation  $\sigma_z$  of road segment and the total number of points  $N$  in the candidate region. The classification is based on this formula (15) [9].

$$f = \alpha * \sigma_z + \gamma/N \quad (15)$$

The candidate region is likely to be road segment region if the objective value,  $f$  of the classifier is smaller than a fixed threshold. As shown in the Fig. 12, the road segment region are series of magenta dot [9].

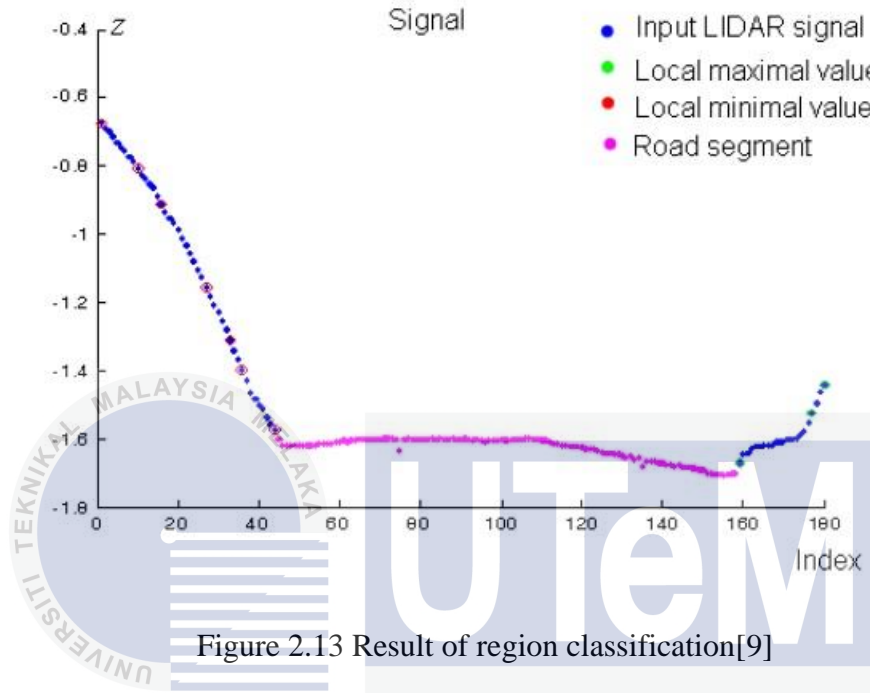


Figure 2.13 Result of region classification[9]

The main reason of false alarm reduction process is to verify potential road regions with minimal road width rule to diminish false alarms. In this system, the threshold value is 4 and it is constant. The width of road regions has to be greater than that value. The distance between two adjacent local points (minimal and maximal) is defined as  $d$ , the road segment width. Finally, the road curb detection process. This process using Hough transform to extract line presentation in the projected points. Using Hough analysis in the top-down view, it provides the curb orientations. The road curb lines are perpendicular to the road surface on the projected plane when the LIDAR sensor scans the road surface. Therefore, to identify the road edges and curbs of the road segment are using curb detection in the top-down view by projecting in the input data on the ground plane [9].

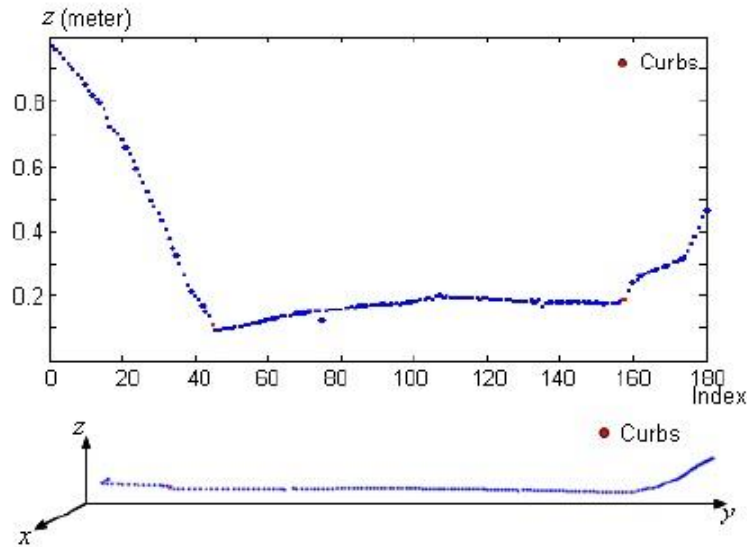


Figure 2.14 Result of road curb detection[9]

The LIDAR sensor has undergone an experiment to test the efficiency of the proposed algorithm. There are two ways of experiment which are the sensor scans the road surface with single scan and multiple scan. In the single scan detection, it detects the road divider and side-walk curb as the road curbs. It also correctly identifies the road segment without confusing with any other obstacles such as vehicles. Hence, multiple scans also produce most road points, road curb points and road edge points correctly. The result comes with a false rate at 0.83% and a miss rate at 0.55%, the errors can be corrected by using Kalman filtering, which is a temporal smoothing technique [9].

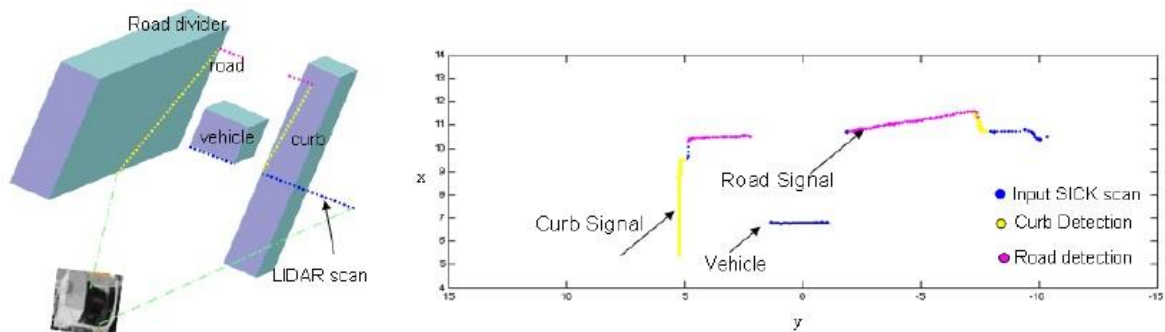


Figure 2.15 Single scan detection result[9]

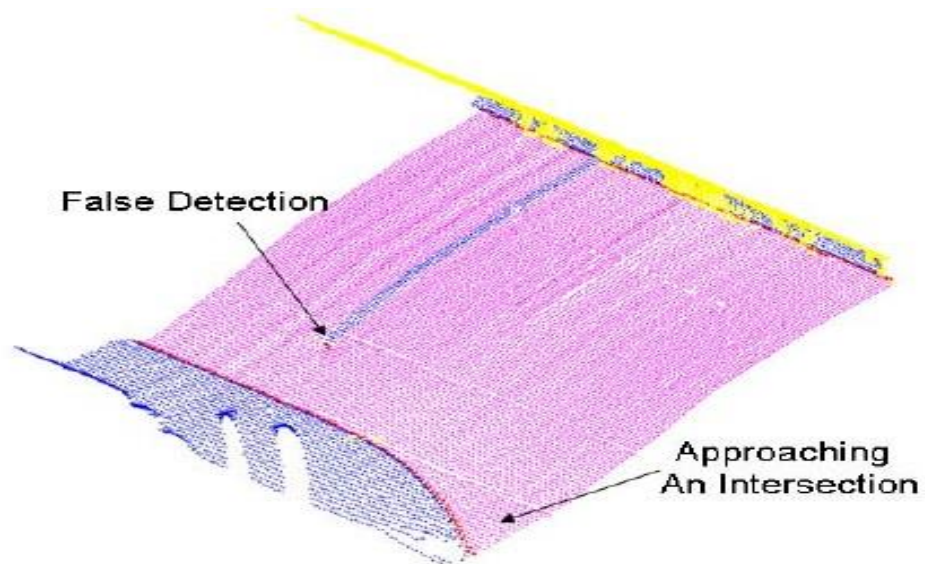


Figure 2.16 Multiple scan detection result[9]



### 2.6.3 Structural Road Detection Based on a 2D Laser Radar

This method has been proposed by Mingyue Feng in his research [11], the method is using laser radar to detect roads but using different approach compared with [8]. The mobile robot may having such trouble in unsmoothed road, in road with irregular edge and running crosswise with the road sign direction in their navigation. The algorithm is named rectangle-searching is proposed to clear up that problems, it based on standard deviation to extract road edge point from road lines [11].

The 2D Laser radar LMS-511 has been used in this method, the basic principle of this is sensor used time of light theory in the measurement of data. The laser pulse is transmit to the object surface and the pulse is reflect back to the LMS-511 laser radar. The distance between the laser radar and the object can be measured using the relationship of the elapsed time. The LMS-511 is equipped with rotating mirror and its enable to scan a plane in the front of the laser radar. The laser radar is installed on the intelligent vehicle with a certain incline angle in downward direction to detect the road. As the laser radar scan the road, it forms a scanning line as the result of it. This paper are focus on scanning on the road with unsmoothed surface, unclear edges and when the vehicle is not parallel with the road [11].



Figure 2.17 An unsmoothed road in radar map[11]

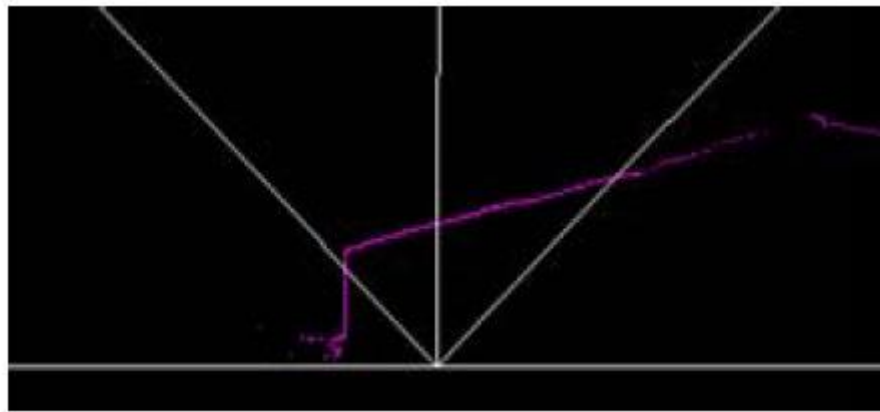


Figure 2.18 An unclear edge on road in radar map[11]

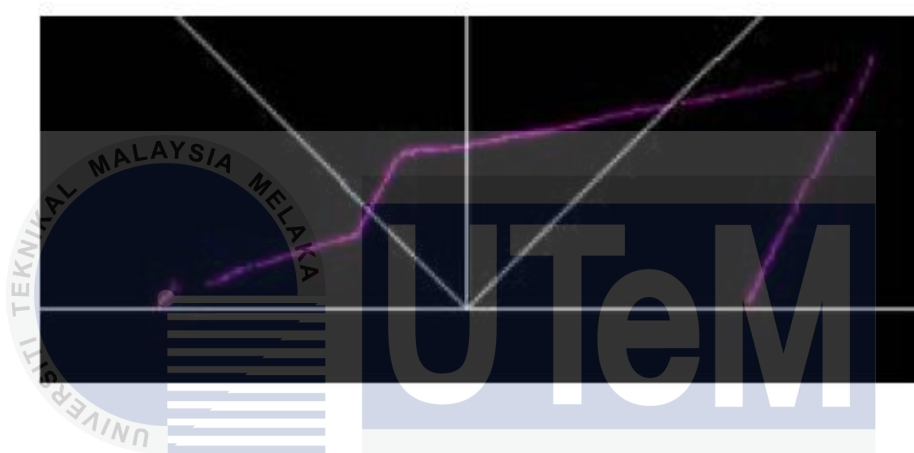


Figure 2.19 Vehicle is not parallel with road in radar map[11]

The rectangle-searching algorithm is focussed on finding the most road points in a rectangle-like square with relatively small width. The crucial task in this algorithm is to find out the most appropriate rectangle to cover the most road contains in the radar points. Fig.19 show the rectangle cover the road points in radar map [11].

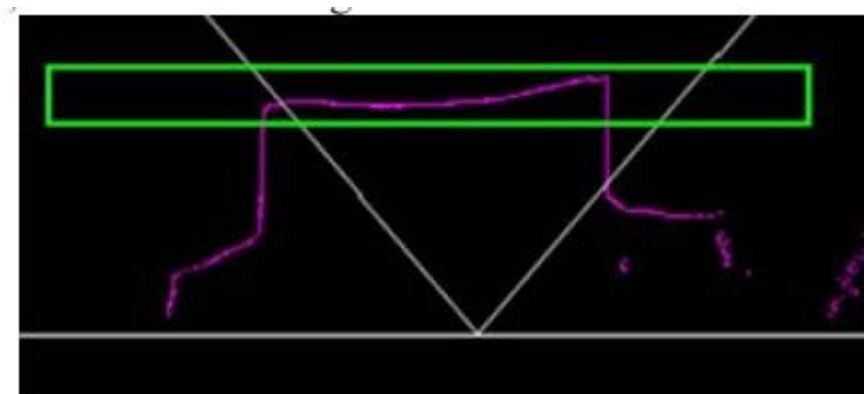


Figure 2.20 Road points covered by the rectangle[11]



Significantly, the laser radar is ensure to suit in nearly all situations in real environment. Hence, the laser radar is setup as shown in Fig.20. From that figure,  $R$  is the position of radar,  $H_r$  is radar height, and  $F$  is represent the middle point in radar detecting series. The width of road, detecting angle of radar and radar's angle resolution are represent by  $W_r, A_r, R_r$  respectively.  $N_r$  is the number of road points detected by radar and  $N_t$  is the number of total radar points. All parameters used in these formula (16) for total number of road points detected by radar and (17) is for total number of radar points [11].

$$N_r = \left\{ \frac{2 \times \arctan\left(\frac{\frac{W_r}{2}}{H_r / \cos(\angle ERO_r)}\right)}{R_r} \right\} \quad (16)$$

$$N_t = A_r / R_r \quad (17)$$

From the calculation, it can conclude that more than half of the total points are reflected back from the road and it is surely that the rectangle can covers the road points [11].

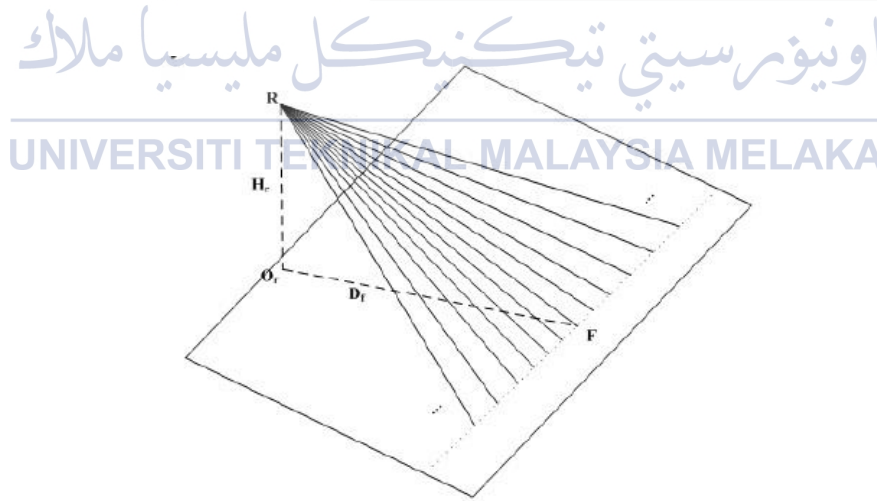


Figure 2.21 Laser radar scanning principle[11]

The formation of the rectangle is used two parallel lines and there a space between represent the width of the rectangle. The length of the rectangle is infinite and changing the line's slope, the width of the rectangular and the beginning point of lower line can produce assorted rectangle to cover the road points [11].



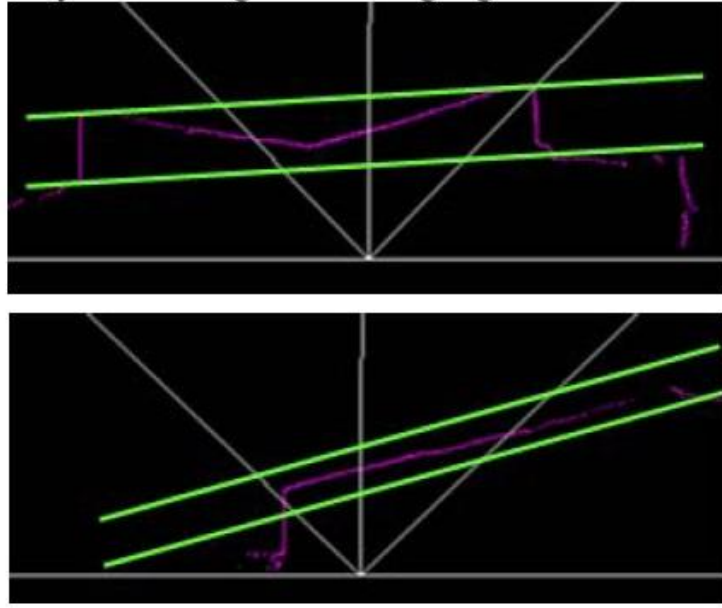


Figure 2.22 Rectangle (green colour) with different slopes cover the road points (magenta colour)[11]

Extraction process the road line from all points inside the rectangle is needed to determine road points and road edge points. The standard deviation of nearby point for short line and long line (two lines have different slope) used as the eigenvalue to differentiate the two type of points. The method of searching for the right endpoint of the road is obtained by using these equation [11].

Assume  $p_s$  and  $p_e$  is the starting point and the ending point of the road. (18) and (19) are the equation for current interval [11].

$$I_t = [s_t, e_t] = \left[ \frac{(p_e + p_s)}{2} - \frac{I}{2}, \frac{(p_e + p_s)}{2} + I/2 \right] \quad (18)$$

$$I_t = [s_t, e_t] = [s_{t-1} + I, e_{t-1} + I] \quad (19)$$

Where  $I_t$  is the current interval,  $I$  is the length of fetched interval and calculate  $D_t$  is the standard deviation of the interval. Add  $t$  by 1. Calculate the current  $D_t$  of this interval. If  $|D_t - D_{t-1}| > K$ , then the right end of the road is found. The algorithm ends and  $e_t$  is to be at the right end of the road; else continue add  $t$  by 1. The process to find the left end of the road is the same [11].

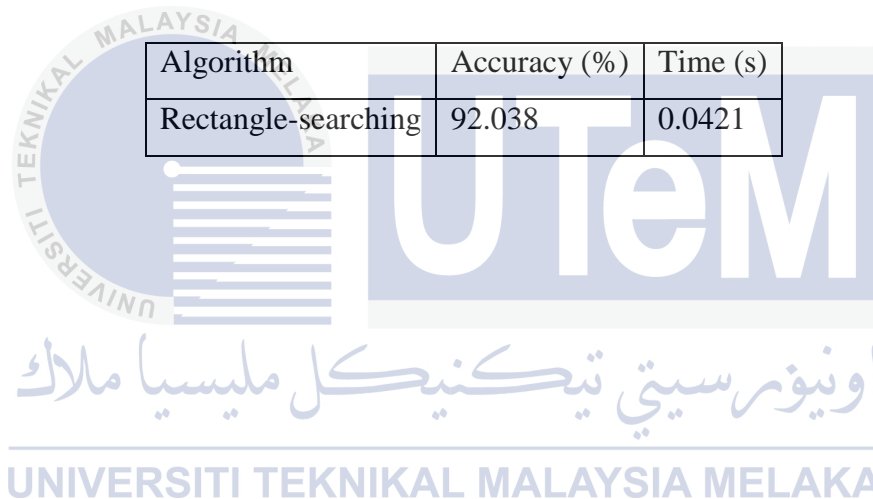
There are two simulations presented using the algorithm in this paper,  $S_1$  and  $S_2$ . The road are flat and have regular road edge in both sides in  $S_1$ . Hence, the road are damaged and unclear edges in  $S_2$ . The evaluation takes on road detecting accuracy and time taken for calculating. From the results, road detection in  $S_1$  is more accurate and take a short time to calculate compared to  $S_2$ . This method also can detect road region in all situations of road surface [11].

Table 2.1 Result for simulation  $S_1$ [11]

Algorithm	Accuracy (%)	Time (s)
Rectangle-searching	95.193	0.0382

Table 2.2 Result in simulation  $S_2$ [11]

Algorithm	Accuracy (%)	Time (s)
Rectangle-searching	92.038	0.0421



#### 2.6.4 Road Edge Detection System using FMCW Radar

The researchers developed a new road edge detection system using frequency-modulated continuous-wave (FMCW) radar in paper [12]. The reason they use a FMCW radar is able to detect more information of road rather than optical images do. The radar technology enable to work efficiently during daylight and night. The radar also can works on any type of ground and in any variety of weather condition. A FMCW basically consists of a voltage-controlled oscillator, a directional power coupler, power amplifiers, a transmitting antenna, a frequency mixer, low pass filters, low noise amplifiers, control data acquisition circuits, a host computer and power supply [12].

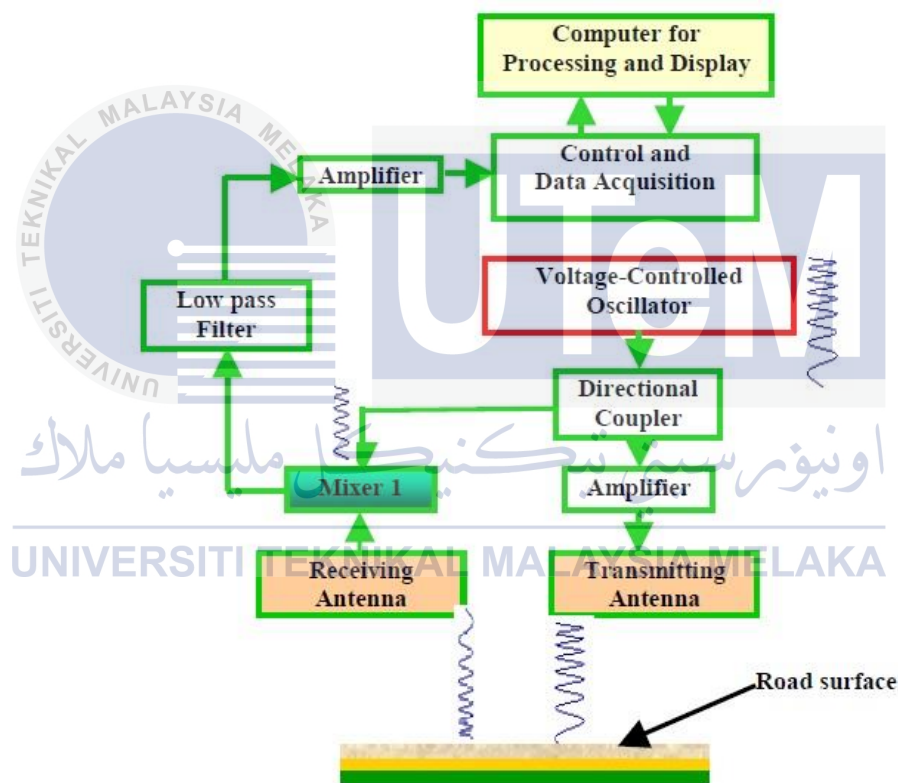


Figure 2.23 Block Diagram of FMCW Radar[12]

In this radar system, a saw-tooth signal act as an input for voltage-controlled oscillator (VCO) and an output is a sinusoidal wave with its frequency linearly modulated. The output frequency of the VCO will increase correspondingly from lower frequency to higher frequency when the magnitude of saw-tooth signal varies from lower level to higher level. A portion of the VCO's output will picks up by the directional coupler and send it to the frequency mixer as a local reference signal. The remainder of VCO's output is send to

the power amplifier to amplify the signal then to be radiated through the transmitting antenna. Part of the wave energy will be reflected back when it hits on the surface of road and picked up by receiving antenna. The frequency mixer mixed the received wave and the local reference wave. These two waves have different frequencies because the road-reflected wave travels a longer distance than the reference wave. The distance from radar to the road surface and the information of the road can be determined by analysing the spectrum of the output signal from the mixer [12].

The scanning technique used in this research is using a single radar because to reduce the cost. The antenna of radar must turn back and forth for covering an angle,  $\theta$  to let the radar beam spot scan from position G to H on the ground. A 2D-profile of the road can be obtained by processing the received reflected signal [12].

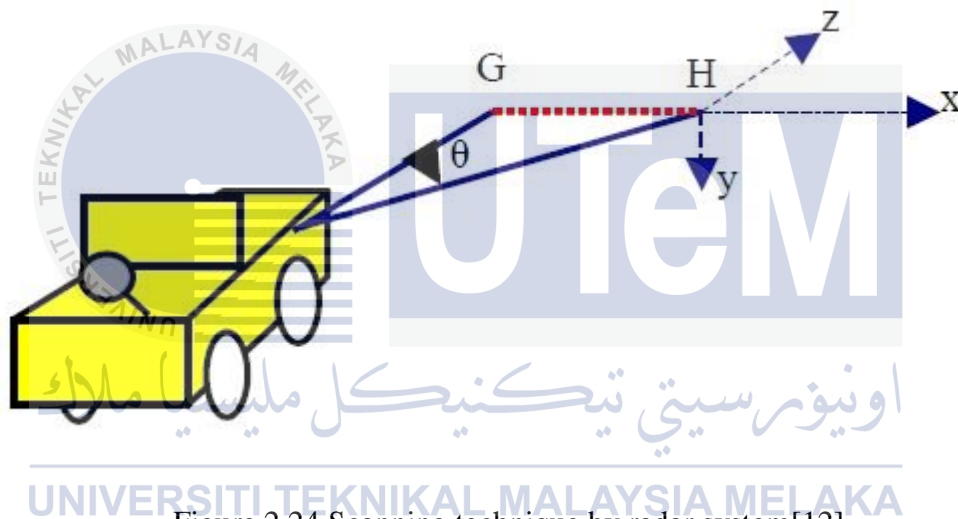


Figure 2.24 Scanning technique by radar system[12]

To test the sensitivity of the FMCW radar in detecting road edge, three tests were setup on the different types of edges. These edges are steep road edge, negative slope road edge and asphalt road shoulder. The FMCW radar is installed on the van and the height is about 12 inches above the road [12].

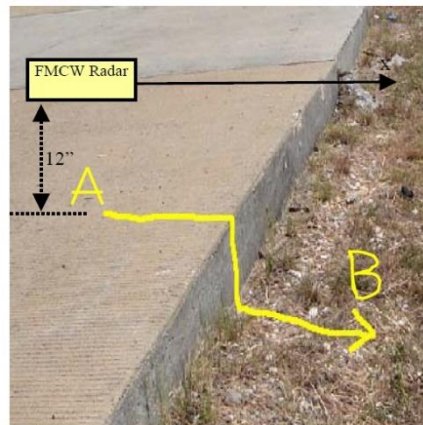


Figure 2.25 Steep road edge road edge [12]

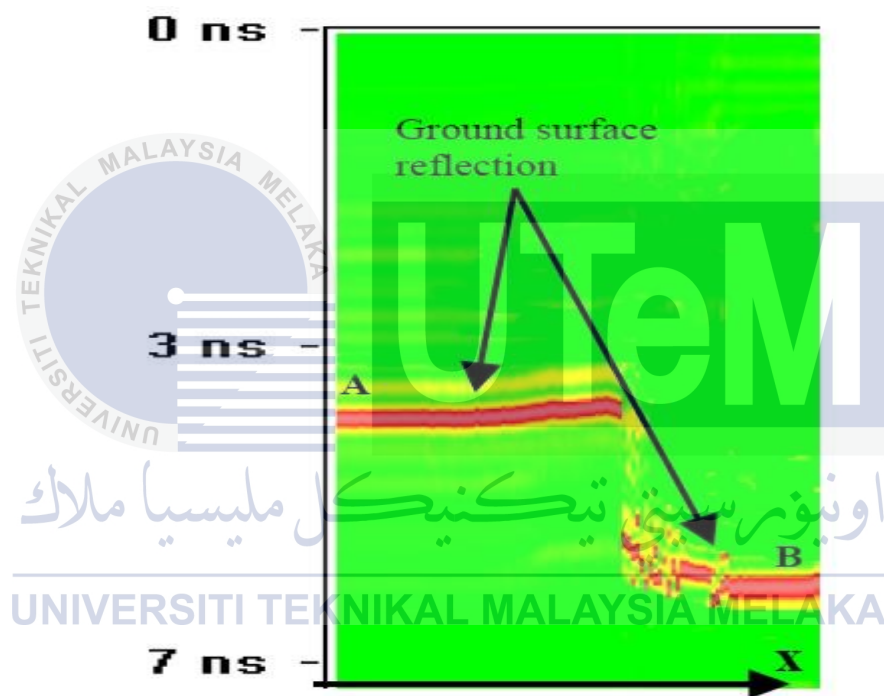


Figure 2.26 Altitude based profile for steep road edge[12]

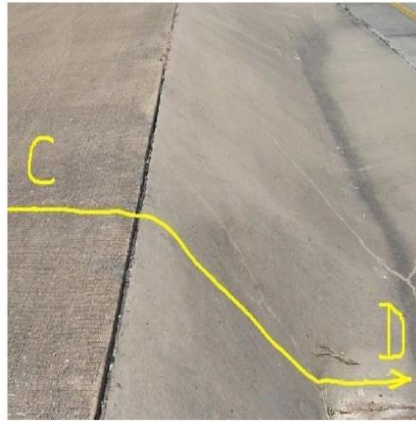


Figure 2.27 Negative slope road edge[12]

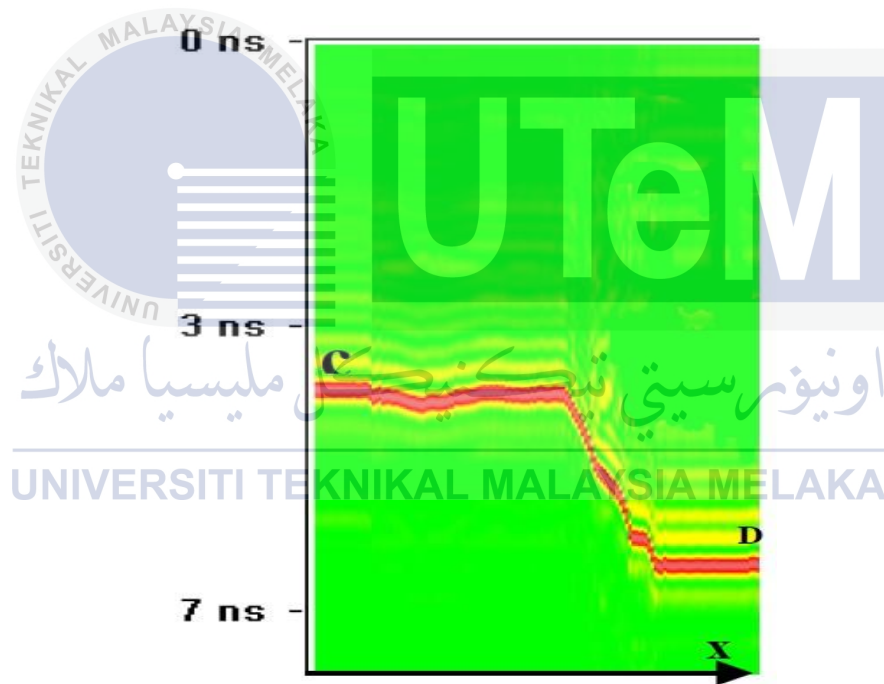


Figure 2.18 Altitude based profile for negative slope road edge[12]



Figure 2.29 Asphalt road shoulder[12]



Figure 2.30 Altitude based profile for asphalt road shoulder[12]

From the result, it demonstrates that the travel time of the surface-reflected wave exactly complement to the altitude of the road surface. It also shows that the different materials of the road will change the reflection intensity but the travel time of the reflected wave is not affected. From Fig.2.29, it shows to detect the boundary between the road and its shoulder. It shows the roughness two different surface and the different of altitude between of them [12].

The system used its position as origin,  $O$  for the relative position of any point on the road surface.  $P(x, y, z)$  is position coordinate where  $x$  is the transverse coordinate,  $y$  is the altitude of the road at that point and  $z$  is the longitudinal coordinate of position  $P$ . In the

measurement process, the radar system send the microwaves to the point  $P$  on the road surface and the received radar signal strength,  $E$  can be determined. The coordinate of point  $P$  and the dielectric constant of the road material also can be solved. The method proposed have demonstrated that the road edge can be detected with FMCW radar, it also can detect road edge even the road may covered by soil, sand or soil [12].





### 2.6.5 Road Boundary Detection Based on Vision

The machine vision method to detect road is a conventional and famously used by the researcher [11]. The method that introduced by Wei Wu and Gong Shu Feng also used the vision method to develop an unstructured road algorithm for road detection [13].

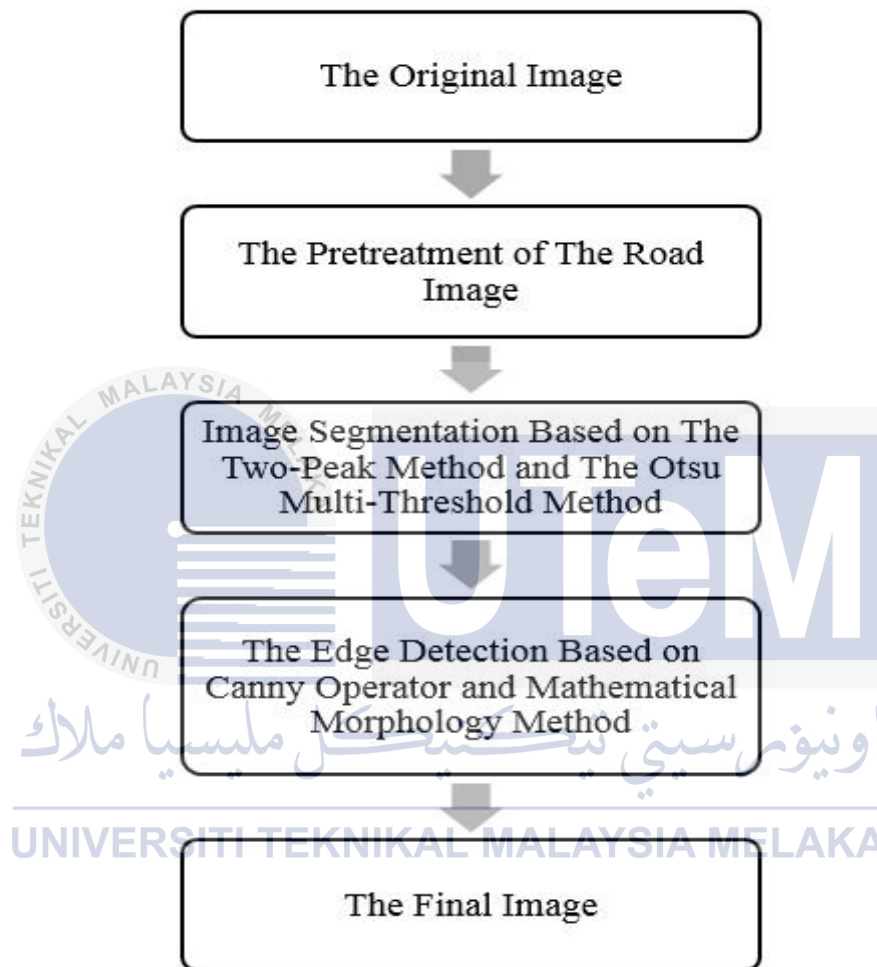


Figure 2.31 Flowchart of road detection[13]

The process started with CCD camera captured the image and carry on with pre-treatment of the primitive image with noise filtration. The researcher choose the medium value filter to do the image pre-treatment [13]. Firstly, the adjacent pixel was sorted according to the gray levels and then choose the intermediate value of this as the template output. Point out that the shape and size of the template window of the two dimensional median value filter have the direct influence for the effect and timeliness. To perform the pre-treatment for the traffic lane image and have a good filter effect, shorten time by using the 3X3 square shape medium value filter template. The image segmentation based on the

two-peak method and Otsu multi-threshold value division algorithm involved complex calculation with a lot of formula. The equation for class variance is (20). The equation for separating factor is (21) and the equation for total variance of the image is (22) [13].

$$\sigma_{BC} = \omega_0(\mu_0 - \mu_T)^2 + \dots + \omega_n(\mu_n - \mu_T)^2 + \dots + \omega_{m-1}(\mu_{m-1} - \mu_T)^2 \quad (20)$$

$$\text{Where, } \omega_0 = \sum_{i=0}^{k_i} P_i, \dots, \omega_n = \sum_{i=k_i+1}^{k_{n+1}} P_i, \dots, \omega_{m-1} = \sum_{i=k_{m-1}+1}^{L-1} P_i$$

$$\mu_0 = \frac{\sum_{i=0}^{k_i} iP_i}{\omega_0}, \dots, \mu_n = \frac{\sum_{i=k_i+1}^{k_{n+1}} iP_i}{\omega_n}, \dots, \mu_{m-1} = \frac{\sum_{i=k_{m-1}+1}^{L-1} iP_i}{\omega_{m-1}}$$

$$\text{Separating factor, } S = \frac{\sigma_{BC}}{v_T} \quad (21)$$

$$\begin{aligned} \text{Total variance of the image, } I \text{ is } v_T \\ = \sum_{i=0}^{L-1} (i - \mu_T)^2 P_i \end{aligned} \quad (22)$$

The edge detection is based on Canny Operator and mathematical morphology method. There a few steps to follow this process, first the image was smoothed using Gaussian filter. Then, the amplitude and direction of the gradient of the smoothed image was determined by calculation. After that, the restrain of the non-maximum value for the amplitude of the gradient to find the partial maximum points of gradient images. The other non-partial maximum points is reset to zero for the refinement edge. Lastly, double thresholds value algorithm used to examine and connect the edge [13].

The foundation of the set theory is used in the mathematics morphology. It used to analyse the image which is the basic of the shape structural elements. The basic principle is to measure and extract the shapes in the image with particular structural element for the image analysis and recognition. This application clarify the data of the image but maintain their basic characteristic of the shape. It also can discard irrelevant structures [13]. In part of

experiment, the setup are the maximum speed of the robot is 3m/s, USB camera as forward visual sensor, 300 thousand pixel images captured with format of 300 x 240 pixels. The most frame number is 30 frames/second [13].



Figure 2.32 The original image of road[13]



Figure 2.33 The final image of road[13]

The result shows that the algorithm for upper road detection is proved for the accuracy and timeliness [13].

## 2.7 Summary of Review

Laser sensor's method is a rapid collecting of measurement data of road boundary recognition and it also provide an accurate measurement of road width [8]. However, the laser sensor is an expensive equipment and need more cost to apply it in this project. Road edge detection method using LIDAR sensor offer an interest in road curb detection [9]. In contrast, this method is only focus in the urban environment where along the road have its curb. Besides, this sensor also a high cost same as the laser sensor. In 2D laser radar, the result shows the validate efficiency and effectiveness in the algorithm [11]. The method used is different in analyse the road points in term of mathematical approach. Furthermore, it is very fast road detection method but it has budget constrain. FMCW radar work effectively under any weather condition like raining and snowing. This method still can detect the road even the line markers or road shoulder are in irregular shape. Besides, this system effectively detect road edge in any shape such as steep road edge and slope road edge [13]. Machine vision is a conventional method in road and road-edge detection [13]. Unfortunately, the machine vision face problems like weather, road covered with sand, soil. This project is proposed to use the ultrasonic sensor as the method of road and road edge detection. The basic idea is using the method of laser sensor in [8] but using a rotating ultrasonic sensor.

## **CHAPTER 3**

### **METHODOLOGY**

#### **3.1 Introduction**

This chapter is about methodology that should be used to do this project. To achieve the objectives of this project, the method, design, sensor parts and experiment procedure need to be done. Two sections are involved in this project's development, hardware and software. The hardware part, the selection of the sensor and motor. The proposed design for the sensor system was also included in this part. Besides, the software part were involved the signal processing and the controller are elaborated. With uses of SolidWorks software, the hardware part was designed and the hardware was fabricated.

UNIVERSITI TEKNIKAL MALAYSIA MELAKA

### 3.2 Process Flow Chart

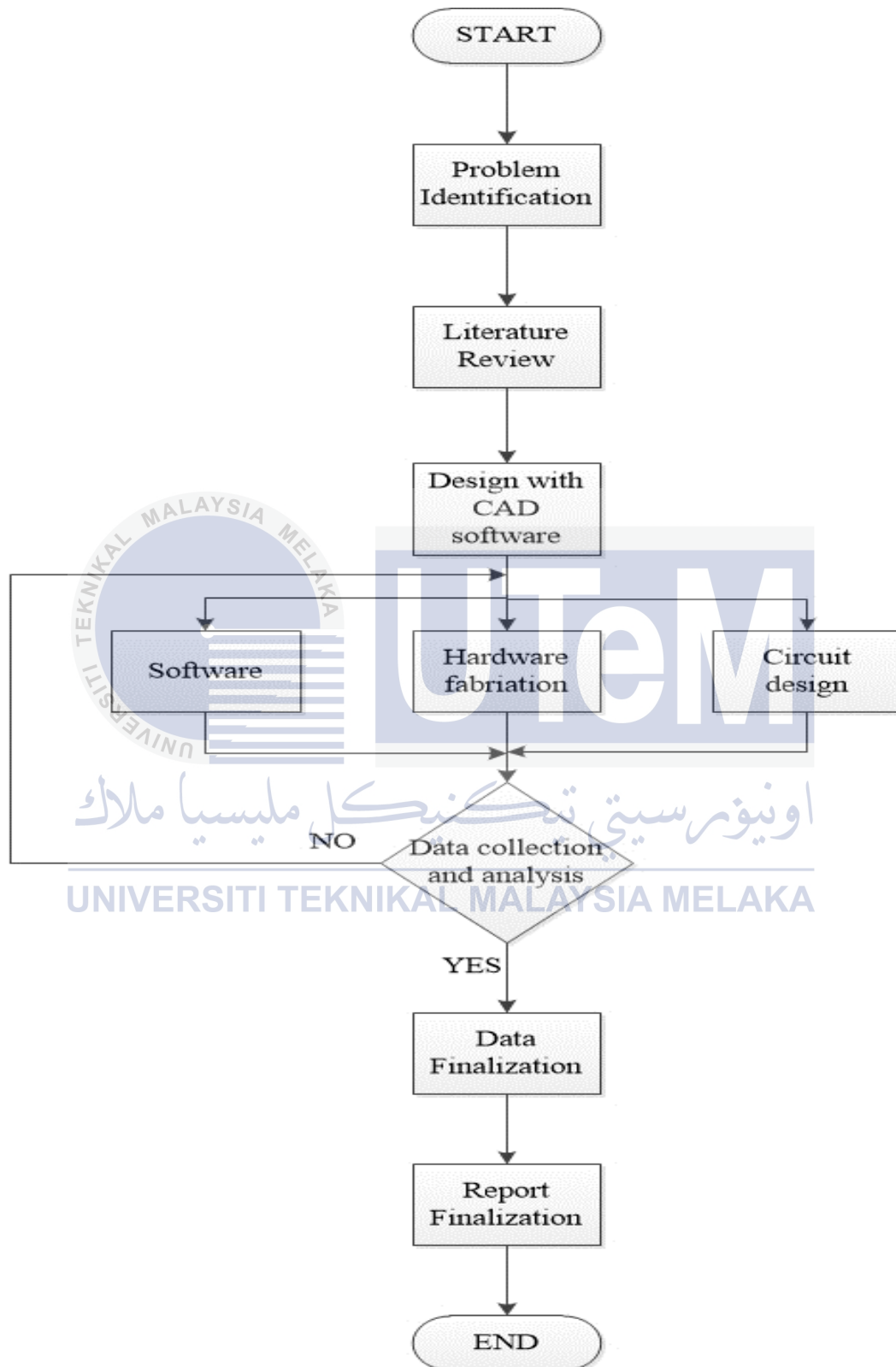


Figure 3.1 PSM flowchart

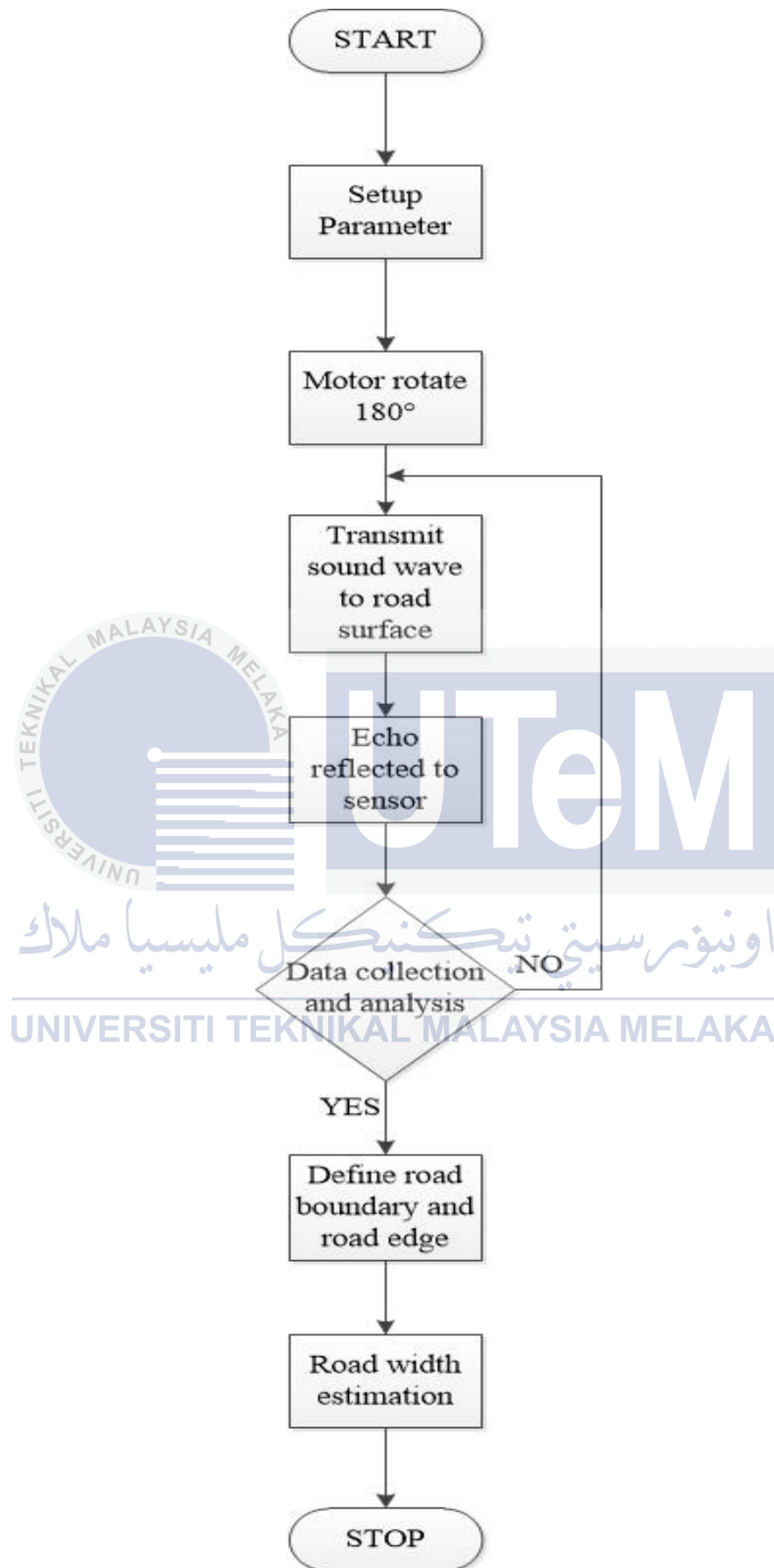


Figure 3.2 Methodology flowchart

Figure 3.2 shows the methodology flowchart of the instrument working to measure road width. Firstly, setup the parameter including measure actual road width, determine the middle point of the road, and connect the sensor to Arduino and to the host computer. Then, motor start rotate  $180^\circ$  ranging on the road surface and the sound wave transmits by the sensor reflected back to the sensor. Next, collect the data and do the analysis including determine the road region and road edge. Then, calculate the road width using data including initial angle of road region, final angle of road region and the distance between the sensor and the road surface.

### 3.3 System Overview

The system is require host computer including Arduino integrated development environment (IDE) software. The Arduino UNO board is act as an interface between input, output and the controller in this system. The ultrasonic sensor's measurement was sent to Arduino board as an input, and send back to host computer as the experiment output.

### 3.4 Hardware Section

In this part, the design was done using SolidWorks software. The SolidWorks software can produce a 3D mechanical computer-aided design. It is a user friendly software with many features to help in the product design. In SolidWorks, it is easier to draw a 3D drawing model compare with other CAD software like AutoCad.

The instrument was designed in two parts, lower part and upper part. The upper part was designed using 2 servo motors. The design was created using pan and tilt concept. Pan is the rotation in the horizontal plane meanwhile tilt is the rotation in the vertical plane. At the top of servo motor, the ultrasonic sensor was placed. The sensor was mounted at  $45^\circ$  from vertical axis (declination angle). Hence, the lower part was designed as a pole and a base. The design was in a cylinder shape with diameter of 2.5 cm for the pole. Whereas, the base was designed in a square shape with length of 40 cm. The sensor is acceptable to be placed on road surface but the surface must be flat. If the surface is not flat, the output will be produced by the sensor may have an error.



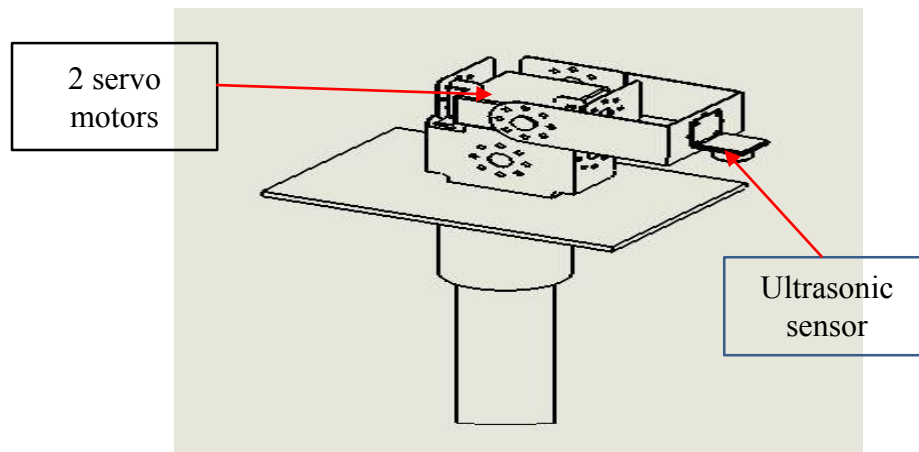


Figure 3.3 Upper part of instrument

### 3.4 Sensor

Ultrasonic sensor was chose to use in this project for road detection. The SN LV-MaxSonar-EZ1 is an ultrasonic sensor produce by Maxbotix. According to the datasheet, this sensor is 42 kHz ultrasonic sensor and it operates from 2.5-5.5V. The resolution for this sensor is 1 inch. The detection range is from 0 inches to 254 inches (6.45 meters), it is possible to detect a whole road width. It is small and light module with 45x20x15 mm of dimensions. Furthermore, it is low cost compared to laser sensor and radar. It provide the interface output formats in pulse width output, analog voltage output and serial digital output. This sensor have 7 pins located on the sensor board. Pin GND is a sensor ground pin. Pin +5V is  $V_{cc}$ , operates on voltage from 2.5V to 5.5V. Pin TX is serial output delivers with an RS232 format. Pin RX is ranging HIGH/LOW for measuring and provide the output data. When HIGH, its allow measuring process while when it LOW, it does not allow the sensor to ranging. The analog output with scaling of  $V_{cc}/512$  per inch. If the power supply is 5V it yields  $\sim 9.8\text{mV/in}$  and it located at Pin AN. Pin PW is the pin outputs for pulse width, to calculate distance scale factor of  $147\mu\text{s}$  per inch [14]. Figure 3.5 show the beam characteristic for SN LV-MaxSonar-EZ1 ultrasonic sensor. In this project, beam pattern D was used to detect road surface and to measure the distance between the sensor and the road surface as the beam pattern D is narrow and straight beam.

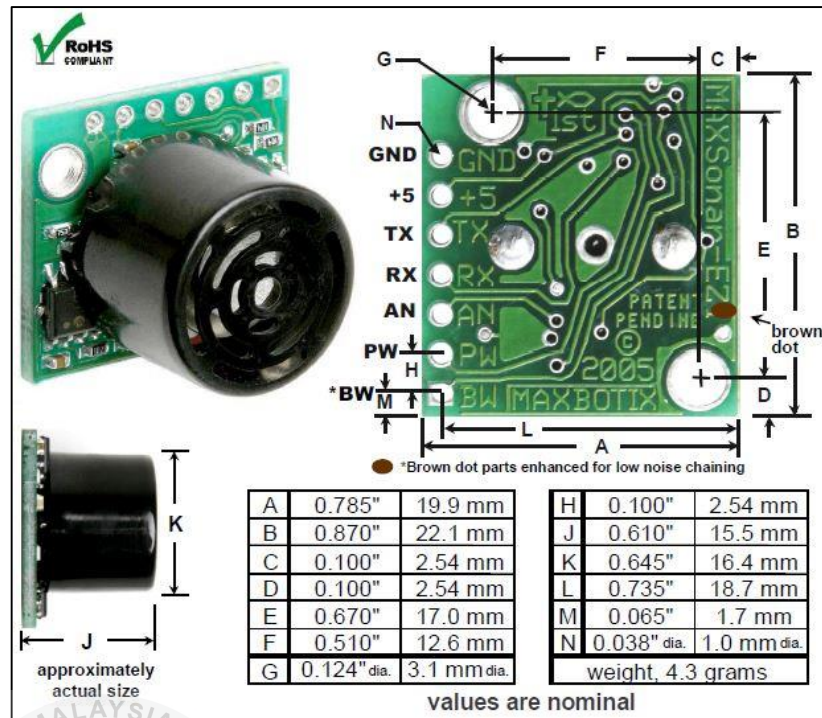


Figure 3.4 SN LV-MaxSonar-EZ1 ultrasonic sensor dimensions

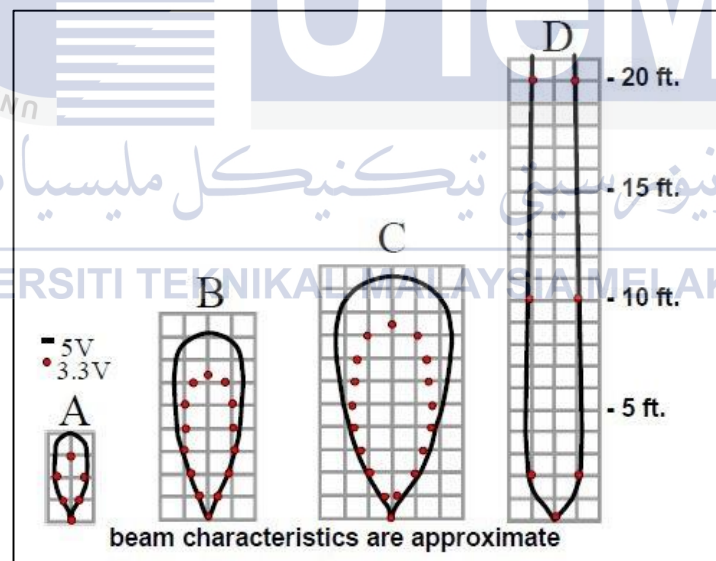


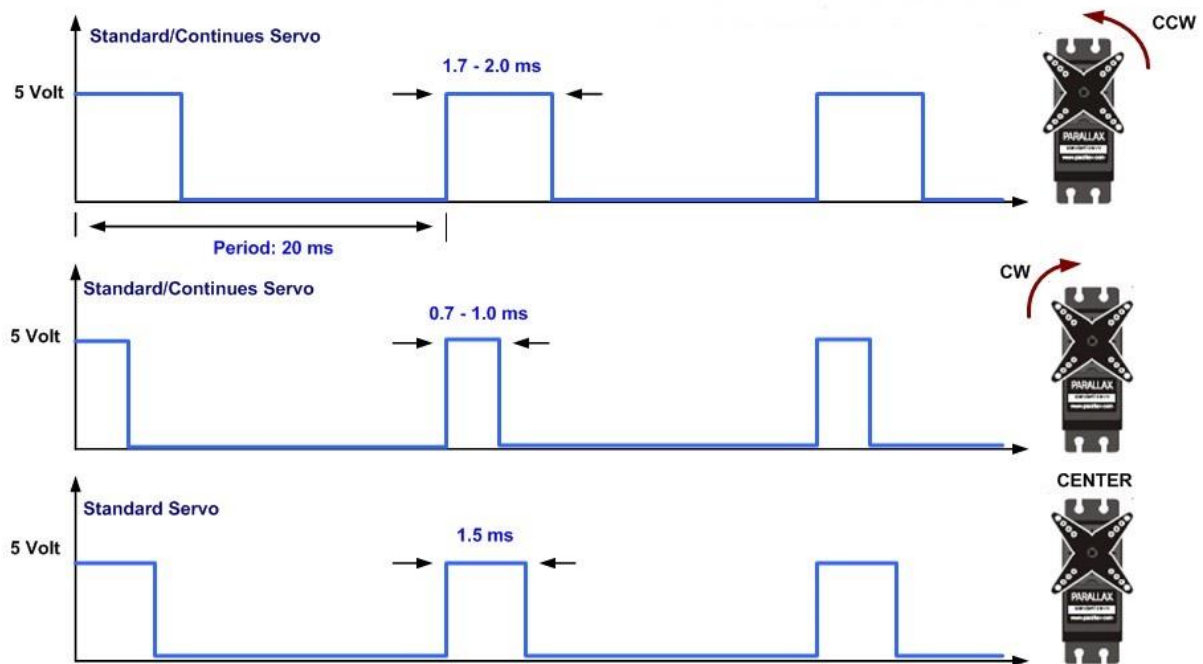
Figure 3.5 Beam characteristic for SN LV-MaxSonar-EZ1 ultrasonic sensor

### 3.5 Motor

The motor was used to rotate the ultrasonic sensor from  $-90^\circ$  to  $+90^\circ$  when ranging the road area. The ultrasonic sensor is equipped at its bracket and connected with shaft through the motor. The bracket and U-joint are used to construct multi-axis joint with the sensor. With help of the bracket and U-joint, the sensor can rotate in 2 motions, pan and tilt. The pan is the rotation in the horizontal plane and the tilt is the rotation in the vertical plane. The servo motor is used for the rotating task. The motor is controlled by sending them a pulse of variable width. The pulse is send through the signal wire. The angle of rotation can be determined by the duration of a pulse that is send to signal wire. It is known as Pulse Width Modulation. The length of the pulse determined how far the motor turns. To make the motor stays in certain position, the position pulse must be repeated to instruct the servo motor [15].



Figure 3.6 Pan-tilt servo motor



Servo Motor PWM Timing Diagram

Figure 3.7 Pulse Width Modulation

### 3.6 Microcontroller

In this project, the Arduino Uno was used as a microcontroller board for data processing unit. It based on the ATmega328 microcontroller. The operating voltage is 5V. It is provides 14 pins as digital input/output pins including 6 pins can be used as PWM outputs. The analog inputs are 6 pins. The ATmega328 has 32 Kb as memory and 2 Kb as SRAM. The EEPROM is 1 Kb. The Arduino Uno is able to communicate with a computer as it have serial communication over USB and it can use as virtual com port to software on the computer. The output signal from the ultrasonic sensor will be sent to Arduino Uno for data processing before send to computer to display the result.



Figure 3.8 Arduino UNO

### 3.7 Hardware of the Ultrasonic Sensor

The ultrasonic sensor was used in this project. This sensor works by transmit the signal to detect the presence of an object or surface then reflect the signal back to the sensor. This sensor was placed at the centre of the body surface. The sensor have 7 pins, Pin GND will connected to ground of the system. Pin +5 will be connected to a 5V power supply. Pin PW is pulse width output from the sensor will be connected to Pin PWM (PWM input) of Arduino Uno board. The outputs from Pin PWM will represent as the distance. The further the distance between road surface and sensor, the higher the output pulse width will produced. In PWM input port of Arduino board, the data will be converted to distance before sends it to computer. To program the microcontroller, the C++ programming will be used. The circuit was developed and simulated using Proteus software to make the hardware works.

### 3.8 Software

Software part plays an important role in this project, processing input to produce the outputs to measure the road width. The sensor is placed on the actuator scans the road 180° repeatedly when it's moving forward along the road. Pin PW at the sensor will transmits

ultrasonic wave to road region to detect road edge. The road surface and road edge will reflect ultrasonic wave and received as an output of the sensor by Pin PW. The process transmitting and receiving the wave will be taken in 0.5 – 1 seconds for each 1° angle of rotation. This is to ensure the wave was completely received by the sensor. The input of the Pin PW on the Arduino UNO is a pulse width modulation and used to read in the pulse that is being sent by the MaxSonar device. The pulse width representation with a scale factor of 147μs per inch. Therefore, this pulse need to be scaled before calculating the range or distance by using equation (23). After that, the range was calculated by using equation (24). The computer with helps of software was plotted the graph and display the road surface profile.

$$\frac{Pulse}{147} = D \quad (23)$$

Where  $D$  is a distance in unit of inch.

$$D \times 2.54 = R \quad (24)$$

Where  $R$  is distance in centimetre.

### 3.9 Experiment and Data Collection

In this part, several experiments were performed to measure the performances of the sensor in reliability and accuracy. The sensor scanning the road 180° repeatedly. Road boundary will reflect the ultrasound wave points when the sensor ranging the road. The time interval will be taken for every 1° of angle. There are 180 times of time interval to complete 180° of angle of rotation. The points are position point of reflected on the road region. The road boundary points are with the smallest distance values between the device and the road surface. There are 3 experiments were conducted to achieve of the objectives of this project.



### 3.9.1 Rotation Speed for Servo Motor Testing

#### Introduction:

First experiment that was conducted is to evaluate the speed of rotation for the servo motor ranging on the road using the road model. The aim of this experiment is to determine the suitable speed for the servo motor to rotate when ranging the road surface. The speed of rotation for servo motor was controlled by using time delay function in Arduino. This function worked to pause the servo motor program in the amount of time before it move again for every  $1^\circ$  of angle. This amount of time delay was also used by the ultrasonic sensor to transmit and receive sound wave when scanning the road surface. The suitable speed was determined by calculate the accuracy of the road model width. The experiment setup is shown below:

#### Experiment variables:

Table 3.1 Experiment variables for Rotation Speed of Servo Motor Experiment

Constant variable	Dimension of road model, Distance between device and road model. Height between device and floor surface.
Manipulated variable	Time delay function for speed of servo motor
Responding variable	Percentage of error for road model width

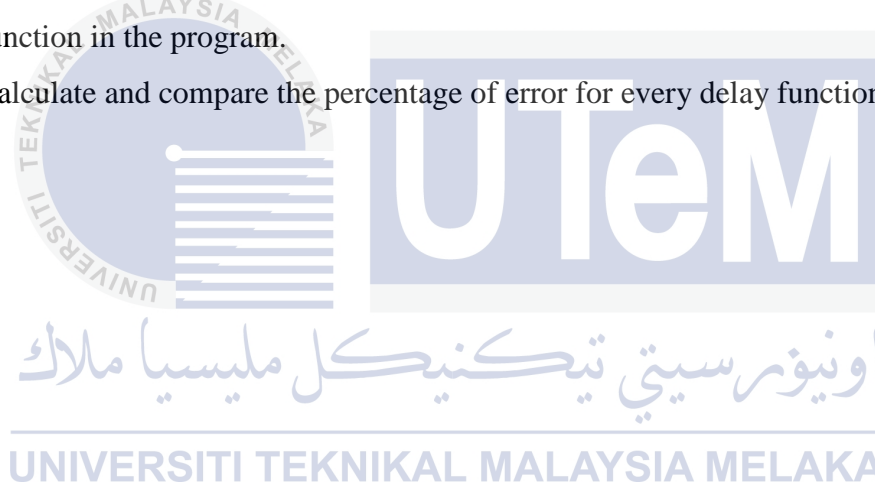
#### Apparatus and Materials:

Arduino Uno, 2 servo motors, ultrasonic sensor, laptop, breadboard, measuring tape, A4 paper box, PVC pipes and masking tapes.

#### Procedures:

1. Build a road model using the A4 paper box. 3 A4 paper boxes are need to build it. Attach the 3 boxes of A4 paper box together using masking tapes. The dimensions of the road model are 92 cm x 23 cm x 23 cm.
2. Place the road model on the floor surface. Make sure the floor surface is flat and clear from any obstacles around it.

3. Measure and record the actual width of the road model using measuring tape. This process was done by using L-shape to ensure the measuring tape was in straight line when measuring the road model width. This step was repeated by 3 times and the average value of the reading were recorded.
4. Place the device in front of the road model. The distance between the device and the road model is 0.5 m. The height between the device and the floor surface is 0.5 m. Make sure the device is placed at the centre of road model.
5. Connect wires from ultrasonic sensor, servo motor to the Arduino board.
6. Connect the Arduino UNO to the laptop and upload the program into the Arduino Uno.
7. Push the switch button and start the experiment.
8. Transfer the data from the serial monitor into Excel and plot the graph.
9. Collect the data for 3 times and repeat the steps 6 - 8 for different time delay function in the program.
10. Calculate and compare the percentage of error for every delay function.





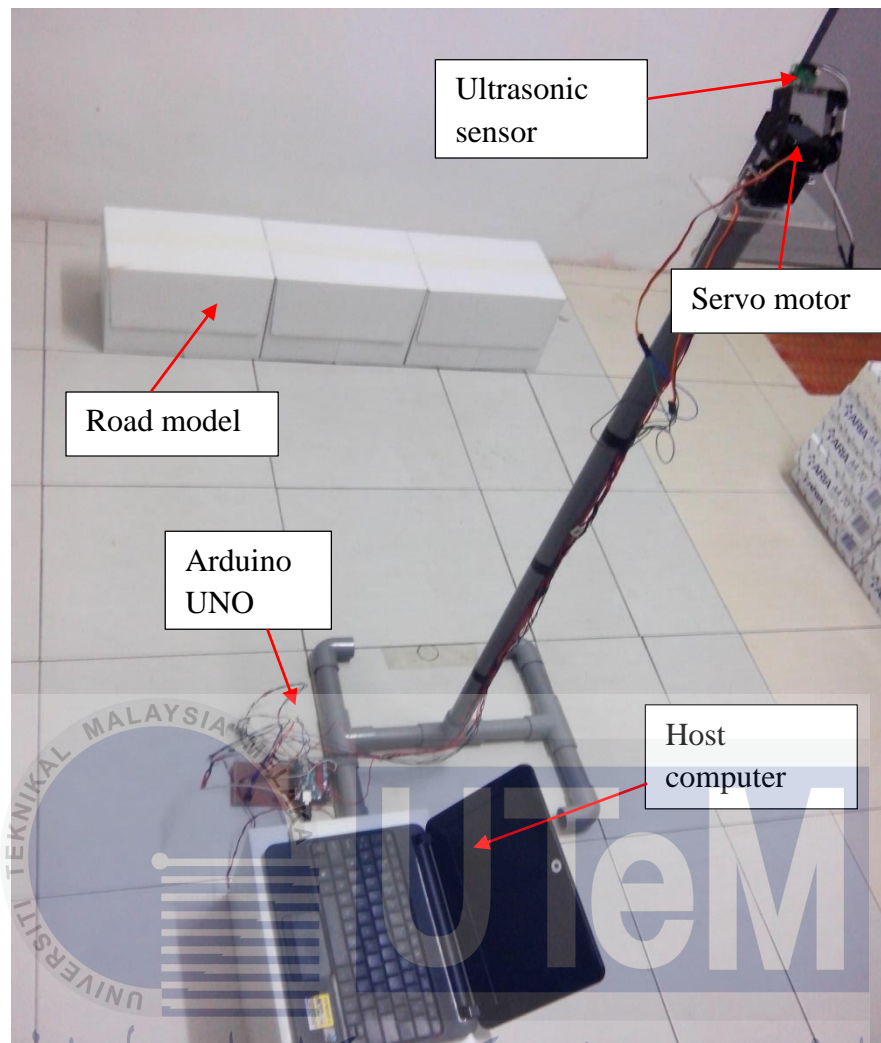


Figure 3.9 Experiment setup on the road model

UNIVERSITI TEKNIKAL MALAYSIA MELAKA

### 3.9.2 Accuracy of Instrument Experiment

Introduction:

Second experiment was conducted to evaluate the accuracy of the road width measured by the instrument. The aim for this experiment to compare with the measured value and the actual value of road width by the percentage of error and the percentage of accuracy. The experiment was conducted on the road with 1 lane and road had road curb along it side. The experiment setup is shown below:

Experiment variables:

Table 3.2 Experiment variables for Accuracy of Instrument Experiment

Constant variable	Time delay function for speed of servo motor, Height between device and road surface.
Manipulated variable	Measured value of road width
Responding variable	Percentage of error and percentage of accuracy for road width

Apparatus and Materials:

Arduino Uno, 2 servo motors, ultrasonic sensor, laptop, measuring tape and road

Procedures:

1. Prepare the instrument and connected to host computer, the road surface must clear and flat before placed the device, because it will affected the scanning process and the output produced.
2. Measure the actual road width using measuring tape and determine the centre point of that road. This process was done by using L-shape to ensure the measuring tape was in straight line when measuring the road width. This step was repeated by 3 times and the average value of the reading were recorded.
3. Place the device on the middle of the road and the height between the device and the road surface is 1 m.
4. Connect wires from ultrasonic sensor, servo motor to the Arduino board.
5. Connect the Arduino UNO to the laptop and upload the program into the Arduino Uno.
6. Push the switch button and start the experiment.
7. Transfer the data from the serial monitor into Excel and plot the graph.
8. Collect the data for 10 times and repeat the steps 6 - 9 for different type of road.
9. Calculate and compare the percentage of error for different type of road to determine the accuracy of the instrument.

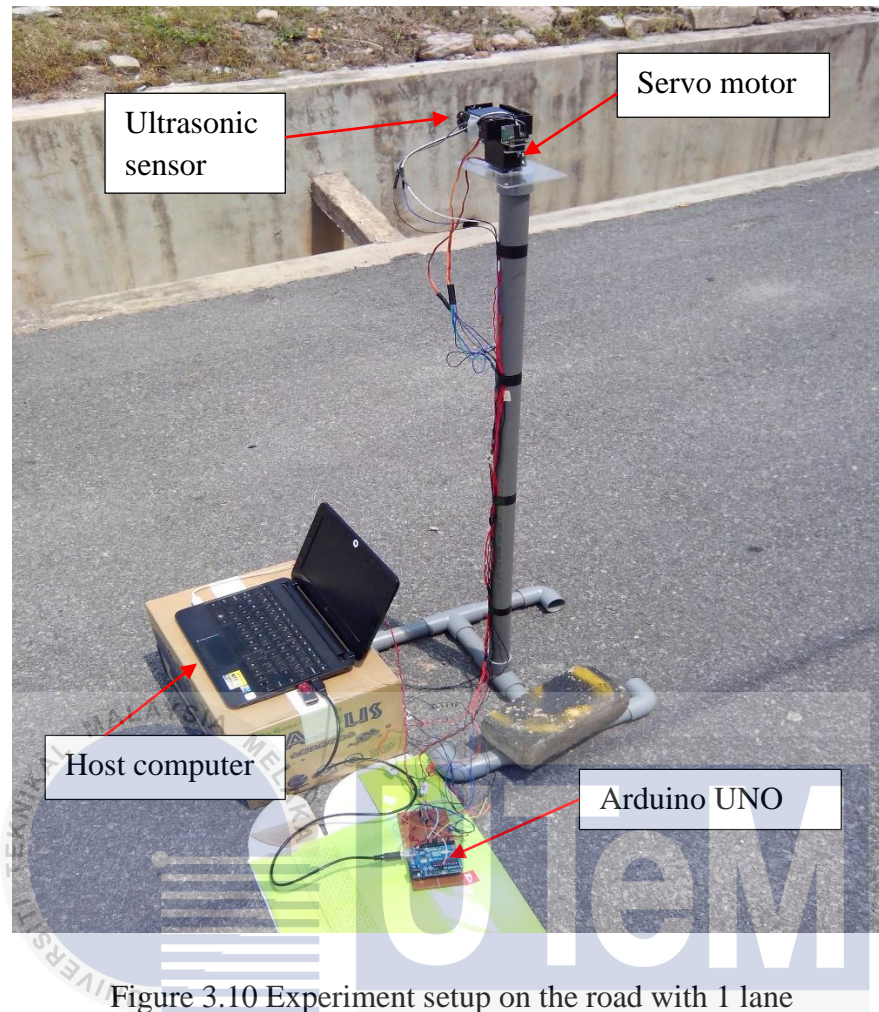


Figure 3.10 Experiment setup on the road with 1 lane

### 3.9.3 Reliability of Instrument Experiment

#### Introduction:

Third experiment was performed to evaluate the reliability of the instrument when compared the road width for road with road shoulder and road with road curbs. The sensor scans the road at both type of roads and the measured value will be collected. The measured value will be compared between both types of roads. The experiment setup is shown below:

Experiment variables:

Table 3.3 Experiment variables for Reliability of Instrument Experiment

Constant variable	Time delay function for speed of servo motor, Height between device and road surface.
Manipulated variable	Measured value of road width
Responding variable	Percentage of error and percentage of accuracy for road model width, Validity of data

Apparatus and Materials:

Arduino Uno, 2 servo motors, ultrasonic sensor, laptop, measuring tape and road

Procedures:

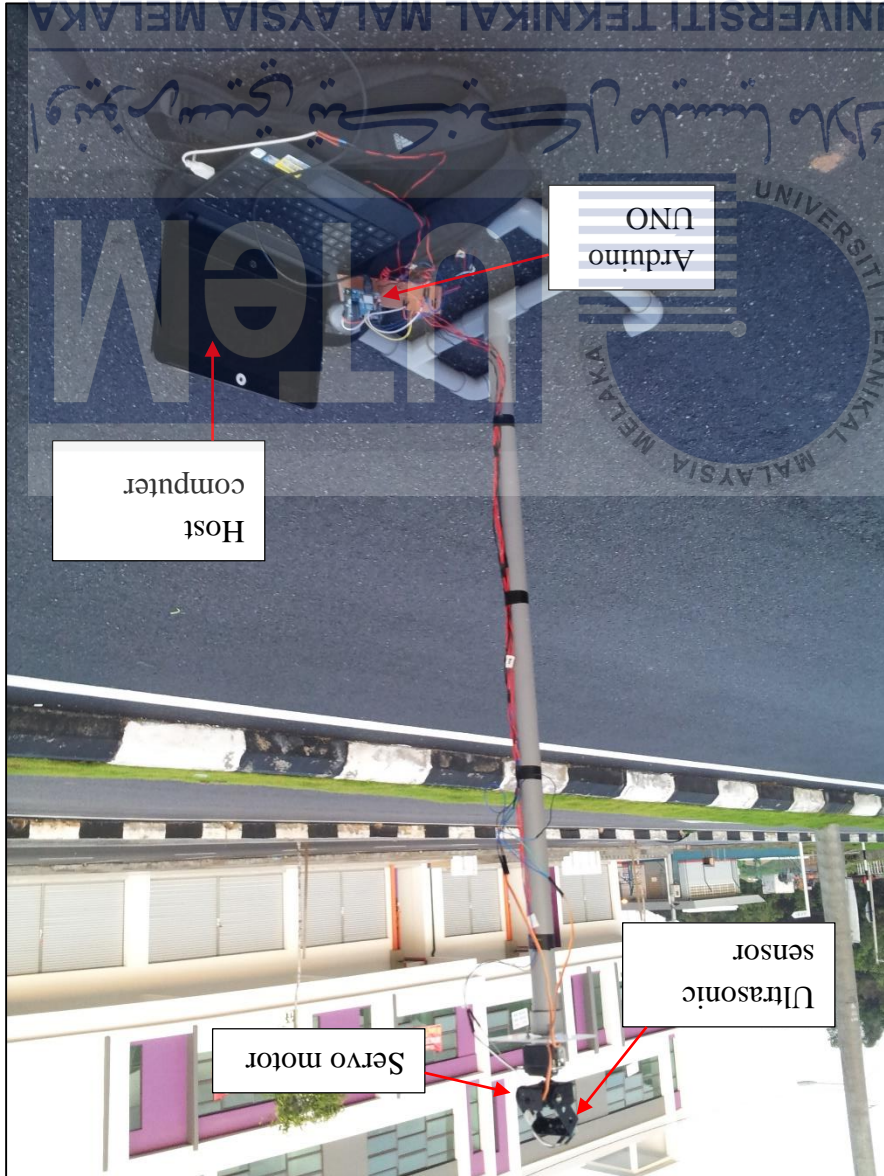
1. Prepare the instrument and connected to host computer, the road surface must clear and flat before placed the device, because it will affected the scanning process and the output produced.
2. Measure the actual road width using measuring tape and determine the centre point of that road. This process was done by using L-shape to ensure the measuring tape was in straight line when measuring the road width. This step was repeated by 3 times and the average value of the reading were recorded.
3. Place the device on the middle of the road and the height between the device and the road surface is 1 m.
4. Connect wires from ultrasonic sensor, servo motor to the Arduino board.
5. Connect the Arduino UNO to the laptop and upload the program into the Arduino Uno.
6. Push the switch button and start the experiment.
7. Transfer the data from the serial monitor into Excel and plot the graph.
8. Collect the data for 30 times and repeat the steps 6 - 9 for different type of road.
9. Calculate and compare the percentage of error for different type of road to determine the accuracy of the instrument.



### 3.10 Summary

In this part, several experiments were performed to measure the performances of the sensor in reliability and accuracy. There are 3 experiments were conducted to achieve of the objectives of this project. The objectives of the experiments were to evaluate the speed of rotation for the servo motor ranging on the road, to evaluate the accuracy of the road width measured by the instrument and to evaluate the reliability of the instrument compared the road width for road had road shoulder and road had road curb. In the experiment, several

Figure 3.11 Experiment setup on the road had road curb



apparatus were needed to perform the experiment such as Arduino Uno, 2 servo motors, ultrasonic sensor, laptop, measuring tape and road. The procedures are to setup the apparatus including connect the instrument to the host computer. Then, measure the actual road width with the measuring tape and determine the middle point of the road. After that, the sensor scanning the road  $180^\circ$  repeatedly. Road boundary will reflect the ultrasound wave points when the sensor ranging the road. The time interval will be taken for every  $1^\circ$  of angle. There are 180 times of time interval to complete  $180^\circ$  of angle of rotation. The points are position point of reflected on the road region. The road boundary points are with the smallest distance values between the device and the road surface. Finally, collect the data to plot the road profile graph, estimate the road width and compare the measured value with the actual value to yield the accuracy and the reliability of the instrument.



## CHAPTER 4

### RESULT AND ANALYSIS

The expected result for this project was to design and develop an instrument to measure road width. The instrument was also tested in several experiments to analyse the accuracy and the reliability of the instrument for measuring the road width.

#### 4.1 Sensor Design

By using the SolidWork software, the design was completed. The instrument was designed in two parts, lower part and upper part. The upper part was designed using 2 servo motors. The design was created using pan and tilt concept. Pan is the rotation in the horizontal plane meanwhile tilt is the rotation in the vertical plane. At the top of servo motor, the ultrasonic sensor was placed. The sensor was mounted at  $45^\circ$  from vertical axis (declination angle). Hence, the lower part was designed as a pole and a base. The pole was designed in a cylinder shape with diameter of 2.5 cm for the pole. Whereas, the base was designed in a square shape with length of 40 cm.



Figure 4.1 Isometric view of sensor

اونيورسيتي تېكنيكل مليسيا ملاك

UNIVERSITI TEKNIKAL MALAYSIA MELAKA



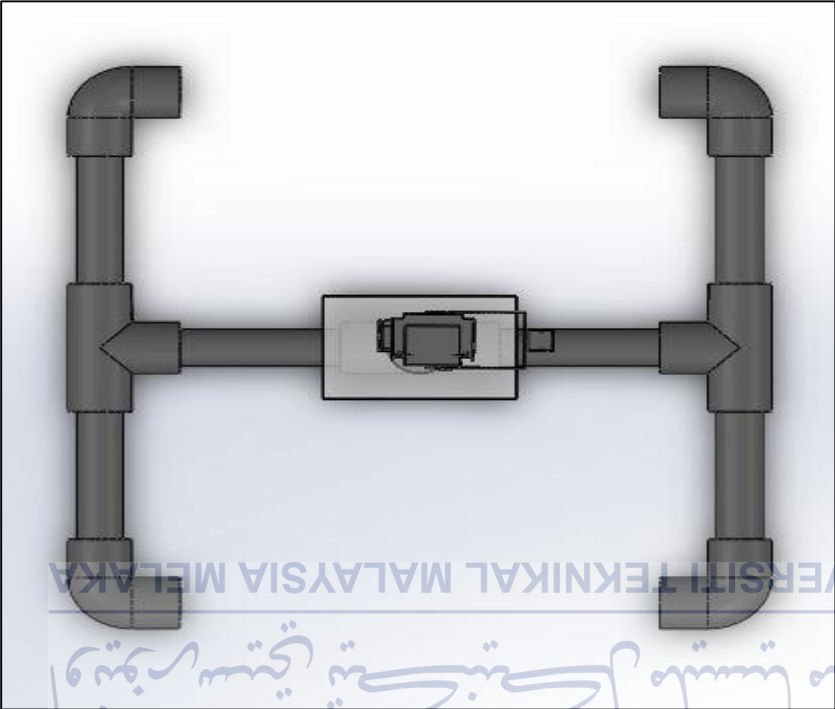


Figure 4.3 Top view of sensor

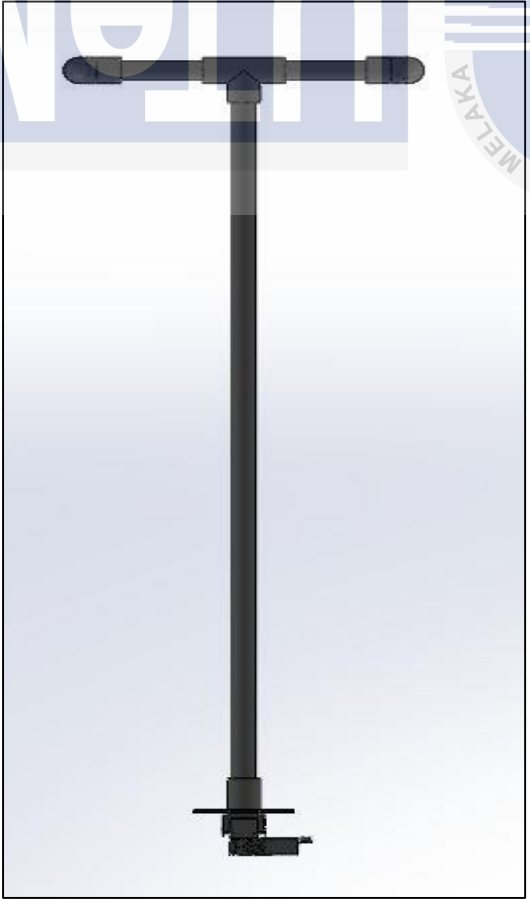


Figure 4.2 Front view of sensor

## 4.2 Data Collection

In this part, the experiments were conducted to test the sensor accuracy and reliability for measuring the road width. The result of the experiments were recorded and analysed.

### 4.2.1 Rotation Speed of Servo Motor Testing

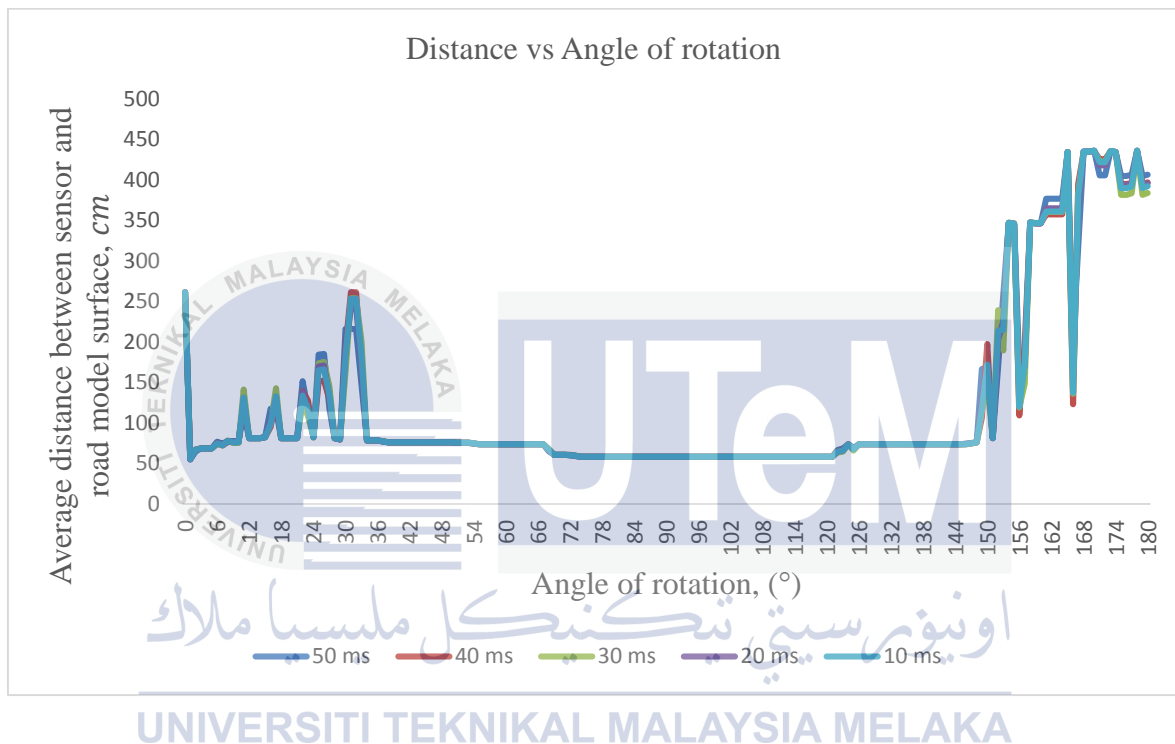
Rotation speed of servo motor is the important part that need to be tested to ensure the sensor can scans all the road region. The rotation speed of servo motor for every 1° degree was controlled using delay function. The time delay functions are 50 *ms*, 40 *ms*, 30 *ms*, 20 *ms*, 10 *ms*. The table shows the data of angle rotation and the distance between the device and the surface of road model. The road profiles were also plotted.

Table 4.1 Average distance between sensor and road model surface for every time delay function.

Angle of rotation, (°)	Average distance between sensor and road model surface, <i>cm</i>				
	50 <i>ms</i>	40 <i>ms</i>	30 <i>ms</i>	20 <i>ms</i>	10 <i>ms</i>
0	261.62	55.88	55.03	193.04	115.99
10	77.89	71.12	112.61	109.22	81.28
20	81.28	81.28	81.28	81.28	81.28
30	215.90	79.59	322.58	164.25	78.74
40	76.20	76.20	76.20	76.20	76.20
50	76.20	76.20	73.66	75.35	73.66
60	73.66	73.66	73.66	73.66	73.66
70	60.96	60.96	59.27	68.58	60.96
80	58.42	58.42	58.42	58.42	58.42
90	58.42	58.42	58.42	58.42	58.42
100	58.42	58.42	58.42	58.42	58.42
110	58.42	58.42	58.42	58.42	58.42
120	58.42	59.27	62.65	58.42	58.42
130	73.66	73.66	73.66	73.66	73.66
140	73.66	73.66	73.66	73.66	73.66

150	168.49	76.20	81.28	77.89	77.89
160	346.29	330.20	309.03	344.59	342.90
170	436.03	375.92	436.88	287.02	374.23
180	406.40	265.01	369.15	374.23	403.86

Figure 4.4 Graph of road model profile for 50 ms, 40 ms, 30 ms, 20 ms, 10 ms time delay functions.



#### 4.2.2 Accuracy Testing

This experiment was conducted to evaluate the accuracy of the road width measured by the instrument. The aim for this experiment to compare with the measured value and the actual value of road width by the percentage of error and the percentage of accuracy. The experiment was conducted on the road with 1 lane and road had road curb along it side. The actual width of road with 1 lane is 4.16 m and the actual width of road had road curb is 7.05 m. The table shows the 10 times of data were taken for angle rotation and the distance between the device and the surface of road. The road profiles were also plotted.

Road with 1 lane:

Table 4.2 Distance between sensor and road surface vs Angle of rotation

Angle of rotation, (°)	Distance between sensor and road surface, <i>cm</i>				
	1 <sup>st</sup> Trial	2 <sup>nd</sup> Trial	3 <sup>rd</sup> Trial	4 <sup>th</sup> Trial	5 <sup>th</sup> Trial
0	12.70	12.70	12.70	12.70	12.70
10	167.64	180.34	180.34	167.64	167.64
20	213.36	228.60	180.34	243.84	165.10
30	220.98	180.34	220.98	231.14	180.34
40	210.82	205.74	208.28	220.98	208.28
50	187.96	185.42	187.96	205.74	167.64
60	175.26	193.04	193.04	226.06	172.72
70	172.72	200.66	175.26	172.72	175.26
80	195.58	193.04	203.20	203.20	172.72
90	193.04	175.26	175.26	175.26	203.20
100	193.04	195.58	220.98	177.80	177.80
110	210.82	185.42	205.74	213.36	157.48
120	213.36	213.36	213.36	213.36	177.80
130	167.64	167.64	167.64	167.64	165.10
140	193.04	193.04	193.04	193.04	190.50
150	195.58	195.58	195.58	193.04	167.64
160	190.50	193.04	190.50	193.04	190.50
170	223.52	223.52	223.52	223.52	223.52
180	223.52	223.52	223.52	223.52	223.52
Angle of rotation, (°)	Distance between sensor and road surface, <i>cm</i>				
	6 <sup>th</sup> Trial	7 <sup>th</sup> Trial	8 <sup>th</sup> Trial	9 <sup>th</sup> Trial	10 <sup>th</sup> Trial
0	12.70	12.70	12.70	12.70	12.70
10	167.64	167.64	167.64	180.34	180.34
20	213.36	243.84	165.10	180.34	228.60
30	220.98	231.14	180.34	220.98	180.34
40	210.82	220.98	208.28	208.28	205.74
50	187.96	205.74	167.64	187.96	185.42
60	175.26	226.06	172.72	193.04	193.04

70	172.72	172.72	175.26	175.26	200.66
80	195.58	203.20	172.72	203.20	193.04
90	193.04	175.26	203.20	175.26	175.26
100	193.04	177.80	177.80	220.98	195.58
110	210.82	213.36	157.48	205.74	185.42
120	213.36	213.36	177.80	213.36	213.36
130	167.64	167.64	165.10	167.64	167.64
140	193.04	193.04	190.50	193.04	193.04
150	195.58	193.04	167.64	195.58	195.58
160	190.50	193.04	190.50	190.50	193.04
170	223.52	223.52	223.52	223.52	223.52
180	223.52	223.52	223.52	223.52	223.52

From the Table 4.2, the average distance for every 10 trials were calculated to plot the road profile as shown below.

Figure 4.5 Graph of road profile for average 10 times of data

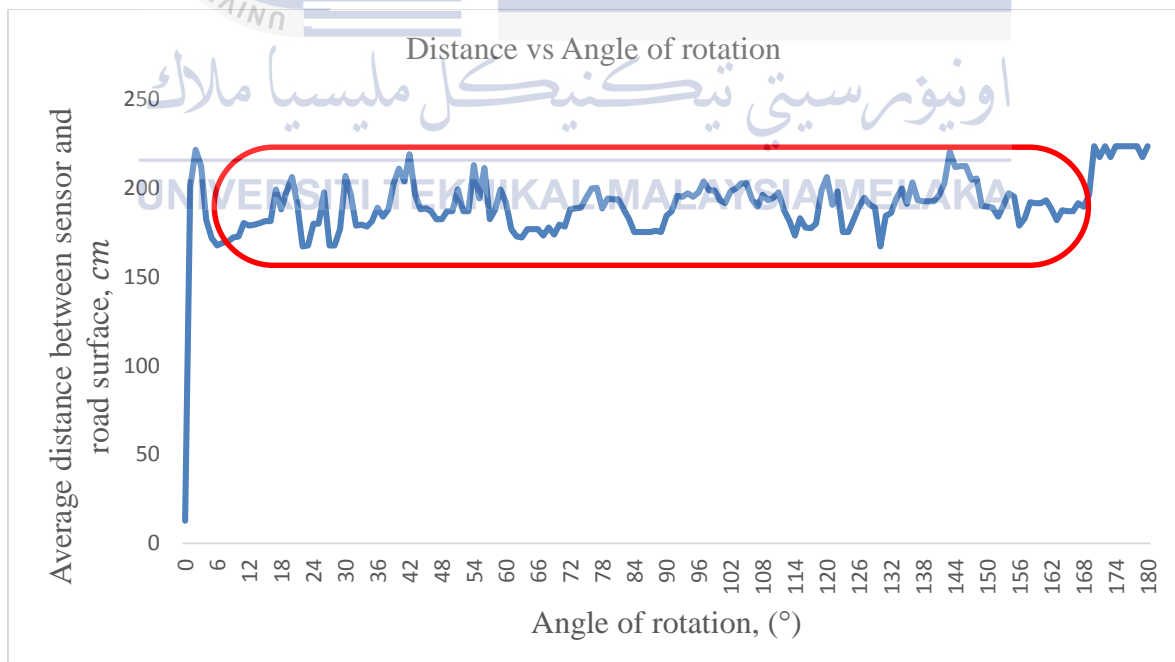


Figure 4.5 shows the road profile for road with 1 lane. Form the graph, it shows the road region of that road inside the red rounded rectangle started at  $6^\circ$  and finished at  $169^\circ$ . The distance between the sensor and the road surface is increase and decrease along the road region in the graph. It is because of the road condition, the road surface is rough. Hence, it effect the sound wave generated by the sensor to reflect in a many directions rather than in a coherent manner. Besides, weather condition also effect the sound propagation between the sensor and the road surface. Windy condition can reduce the sound speed hence its effect the measured value of the road width.

Road had road curb:

Table 4.3 Distance between sensor and road surface vs Angle of rotation

Angle of rotation, ( $^\circ$ )	Distance between sensor and road surface, <i>cm</i>				
	1 <sup>st</sup> Trial	2 <sup>nd</sup> Trial	3 <sup>rd</sup> Trial	4 <sup>th</sup> Trial	5 <sup>th</sup> Trial
0	17.78	17.79	15.24	12.7	12.7
10	363.22	363.22	363.22	365.76	363.22
20	365.76	365.76	365.76	365.76	365.76
30	325.50	325.50	325.50	325.50	325.50
40	325.50	325.50	325.50	325.50	325.50
50	325.50	325.50	325.50	325.50	325.50
60	325.50	325.50	325.50	325.50	325.50
70	325.50	325.50	325.50	325.50	325.50
80	325.50	325.50	325.50	325.9	325.50
90	325.50	325.50	325.50	325.9	325.50
100	325.50	325.50	325.50	337.8	325.50
110	325.50	325.50	345.42	345.42	325.50
120	325.50	325.50	325.50	325.50	331.62
130	325.50	325.50	325.50	325.50	325.50
140	325.50	325.50	325.50	318.44	325.50
150	325.50	325.50	325.50	325.50	325.50
160	325.50	320.98	325.50	325.50	325.50
170	363.22	363.22	363.22	363.22	360.68
180	363.22	360.68	360.68	363.22	363.22

Angle of rotation, (°)	Distance between sensor and road surface, <i>cm</i>				
	6 <sup>th</sup> Trial	7 <sup>th</sup> Trial	8 <sup>th</sup> Trial	9 <sup>th</sup> Trial	10 <sup>th</sup> Trial
0	12.7	17.77	17.79	12.7	12.7
10	365.76	365.76	365.76	363.22	363.22
20	365.76	365.76	363.22	325.50	365.76
30	325.50	325.50	325.50	325.50	325.5
40	325.50	325.50	325.50	325.50	325.5
50	325.50	325.50	325.50	325.50	325.5
60	325.50	325.50	325.50	325.50	325.5
70	325.50	325.50	325.50	325.50	325.5
80	325.50	325.50	325.50	325.50	325.5
90	325.50	315.90	325.50	325.50	325.5
100	325.50	317.80	336.06	325.50	325.5
110	338.76	325.50	325.50	336.22	325.5
120	325.50	325.50	341.62	325.50	325.5
130	325.50	325.50	325.50	325.50	325.5
140	325.50	320.98	325.50	325.50	325.5
150	310.82	325.50	325.50	310.82	325.5
160	325.50	325.50	325.50	325.50	325.5
170	363.22	363.98	363.22	363.22	363.22
180	363.22	363.22	363.22	363.22	363.22

From the Table 4.3, the average distance for every 10 trials were calculated to plot the road profile as shown below.

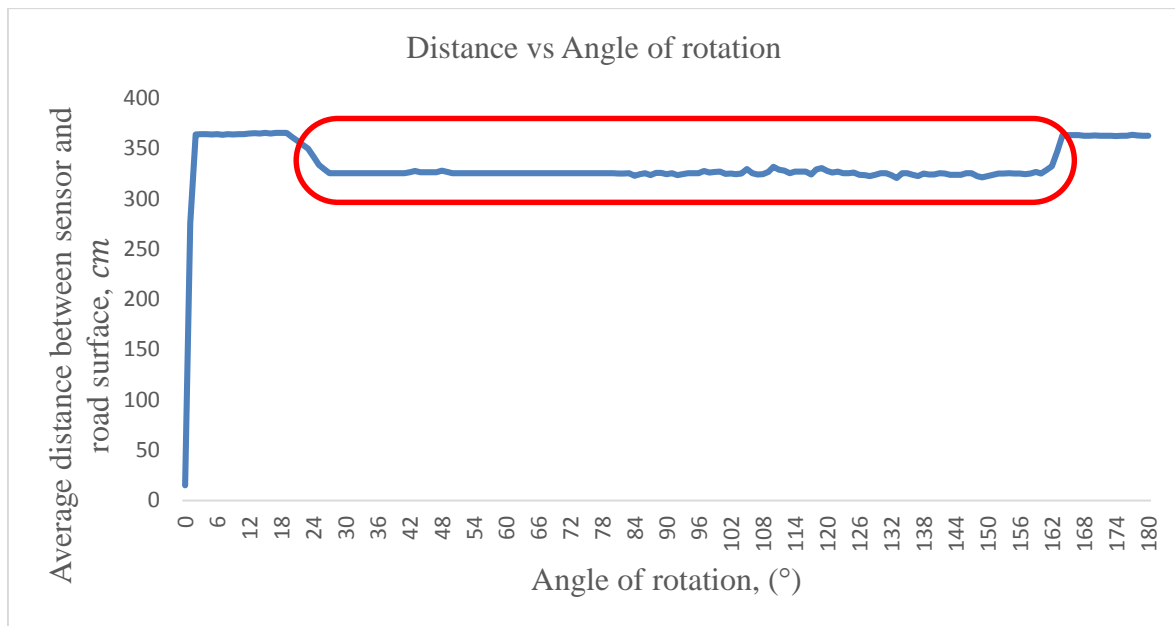


Figure 4.6 Graph of road profile for average 10 times of data

Figure 4.6 shows the road profile for road had road curb along it side. From the graph, it shows the road region of that road inside the red rounded rectangle started at 27° and finished at 162°. The distance between the sensor and the road surface is steadily along the road region in the graph. It is because of the road condition, the road surface is smooth. Hence, it effect the sound wave generated by the sensor to reflect in a coherent manner.

UNIVERSITI TEKNIKAL MALAYSIA MELAKA

#### 4.2.3 Reliability Testing

Third experiment was performed to evaluate the reliability of the instrument when compared the road width for road with road shoulder and road with road curbs. The sensor scans the road at both type of roads and the measured value will be collected. The measured value will be compared between both types of roads. The actual width of road with 1 lane is 4.16 m and the actual width of road had road curb is 7.05 m.



Road with 1 lane:

Table 4.4 Distance between sensor and road surface for 30 trials

Angle, (°)	Distance between sensor and road surface, <i>cm</i>									
	1 <sup>st</sup> Trial	2 <sup>nd</sup> Trial	3 <sup>rd</sup> Trial	4 <sup>th</sup> Trial	5 <sup>th</sup> Trial	6 <sup>th</sup> Trial	7 <sup>th</sup> Trial	8 <sup>th</sup> Trial	9 <sup>th</sup> Trial	10 <sup>th</sup> Trial
0	12.70	12.70	12.70	12.70	12.70	12.70	12.70	12.70	12.70	12.70
10	167.64	180.34	180.34	167.64	167.64	167.64	167.64	167.64	180.34	180.34
20	213.36	228.60	180.34	243.84	165.10	213.36	243.84	165.10	180.34	228.60
30	220.98	180.34	220.98	231.14	180.34	220.98	231.14	180.34	220.98	180.34
40	210.82	205.74	208.28	220.98	208.28	210.82	220.98	208.28	208.28	205.74
50	187.96	185.42	187.96	205.74	167.64	187.96	205.74	167.64	187.96	185.42
60	175.26	193.04	193.04	226.06	172.72	175.26	226.06	172.72	193.04	193.04
70	172.72	200.66	175.26	172.72	175.26	172.72	172.72	175.26	175.26	200.66
80	195.58	193.04	203.20	203.20	172.72	195.58	203.20	172.72	203.20	193.04
90	193.04	175.26	175.26	175.26	203.20	193.04	175.26	203.20	175.26	175.26
100	193.04	195.58	220.98	177.80	177.80	193.04	177.80	177.80	220.98	195.58
110	210.82	185.42	205.74	213.36	157.48	210.82	213.36	157.48	205.74	185.42
120	213.36	213.36	213.36	213.36	177.80	213.36	213.36	177.80	213.36	213.36
130	167.64	167.64	167.64	167.64	165.10	167.64	167.64	165.10	167.64	167.64
140	193.04	193.04	193.04	193.04	190.50	193.04	193.04	190.50	193.04	193.04
150	195.58	195.58	195.58	193.04	167.64	195.58	193.04	167.64	195.58	195.58
160	190.50	193.04	190.50	193.04	190.50	190.50	193.04	190.50	190.50	193.04
170	223.52	223.52	223.52	223.52	223.52	223.52	223.52	223.52	223.52	223.52
180	223.52	223.52	223.52	223.52	223.52	223.52	223.52	223.52	223.52	223.52
Angle, (°)	Average distance between sensor and road surface, <i>cm</i>									
	11 <sup>st</sup> Trial	12 <sup>nd</sup> Trial	13 <sup>rd</sup> Trial	14 <sup>th</sup> Trial	15 <sup>th</sup> Trial	16 <sup>th</sup> Trial	17 <sup>th</sup> Trial	18 <sup>th</sup> Trial	19 <sup>th</sup> Trial	20 <sup>th</sup> Trial
0	12.70	12.70	12.70	12.70	12.70	12.70	12.70	12.70	12.70	12.70
10	167.64	180.34	180.34	167.64	167.64	167.64	167.64	167.64	180.34	180.34
20	213.36	228.60	180.34	243.84	165.10	213.36	243.84	165.10	180.34	228.60
30	220.98	180.34	220.98	231.14	180.34	220.98	231.14	180.34	220.98	180.34
40	210.82	205.74	208.28	220.98	208.28	210.82	220.98	208.28	208.28	205.74
50	187.96	185.42	187.96	205.74	167.64	187.96	205.74	167.64	187.96	185.42
60	175.26	193.04	193.04	226.06	172.72	175.26	226.06	172.72	193.04	193.04
70	172.72	200.66	175.26	172.72	175.26	172.72	172.72	175.26	175.26	200.66
80	195.58	193.04	203.20	203.20	172.72	195.58	203.20	172.72	203.20	193.04
90	193.04	175.26	175.26	175.26	203.20	193.04	175.26	203.20	175.26	175.26



Road had road curb:

Table 4.5 Distance between sensor and road surface for 30 trials

Angle, (°)	Distance between sensor and road surface, <i>cm</i>									
	1 <sup>st</sup> Trial	2 <sup>nd</sup> Trial	3 <sup>rd</sup> Trial	4 <sup>th</sup> Trial	5 <sup>th</sup> Trial	6 <sup>th</sup> Trial	7 <sup>th</sup> Trial	8 <sup>th</sup> Trial	9 <sup>th</sup> Trial	10 <sup>th</sup> Trial
0	17.78	17.79	15.24	12.70	12.70	12.70	17.77	17.79	12.70	12.70
10	363.22	363.22	363.22	365.76	363.22	365.76	365.76	365.76	363.22	363.22
20	365.76	365.76	365.76	365.76	365.76	365.76	365.76	363.22	325.50	365.76
30	325.50	325.50	325.50	325.50	325.50	325.50	325.50	325.50	325.50	325.50
40	325.50	325.50	325.50	325.50	325.50	325.50	325.50	325.50	325.50	325.50
50	325.50	325.50	325.50	325.50	325.50	325.50	325.50	325.50	325.50	325.50
60	325.50	325.50	325.50	325.50	325.50	325.50	325.50	325.50	325.50	325.50
70	325.50	325.50	325.50	325.50	325.50	325.50	325.50	325.50	325.50	325.50
80	325.50	325.50	325.50	325.90	325.50	325.50	325.50	325.50	325.50	325.50
90	325.50	325.50	325.50	325.90	325.50	325.50	315.90	325.50	325.50	325.50
100	325.50	325.50	325.50	337.80	325.50	325.50	317.80	336.06	325.50	325.50
110	325.50	325.50	345.42	345.42	325.50	338.76	325.50	325.50	336.22	325.50
120	325.50	325.50	325.50	325.50	331.62	325.50	325.50	341.62	325.50	325.50
130	325.50	325.50	325.50	325.50	325.50	325.50	325.50	325.50	325.50	325.50
140	325.50	325.50	325.50	318.44	325.50	325.50	320.98	325.50	325.50	325.50
150	325.50	325.50	325.50	325.50	325.50	310.82	325.50	325.50	310.82	325.50
160	325.50	320.98	325.50	325.50	325.50	325.50	325.50	325.50	325.50	325.50
170	363.22	363.22	363.22	363.22	360.68	363.22	363.98	363.22	363.22	363.22
180	363.22	360.68	360.68	363.22	363.22	363.22	363.22	363.22	363.22	363.22
Angle, (°)	Average distance between sensor and road surface, <i>cm</i>									
	11 <sup>st</sup> Trial	12 <sup>nd</sup> Trial	13 <sup>rd</sup> Trial	14 <sup>th</sup> Trial	15 <sup>th</sup> Trial	16 <sup>th</sup> Trial	17 <sup>th</sup> Trial	18 <sup>th</sup> Trial	19 <sup>th</sup> Trial	20 <sup>th</sup> Trial
0	12.70	17.79	12.70	17.77	12.70	12.70	12.70	17.79	15.24	17.78
10	363.22	365.76	363.22	365.76	363.22	365.76	365.76	363.22	363.22	363.22
20	365.76	363.22	325.50	365.76	365.76	365.76	365.76	365.76	365.76	365.76
30	325.50	325.50	325.50	325.50	325.50	325.50	325.50	325.50	325.50	325.50
40	325.50	325.50	325.50	325.50	325.50	325.50	325.50	325.50	325.50	325.50
50	325.50	325.50	325.50	325.50	325.50	325.50	325.50	325.50	325.50	325.50
60	325.50	325.50	325.50	325.50	325.50	325.50	325.50	325.50	325.50	325.50
70	325.50	325.50	325.50	325.50	325.50	325.50	325.50	325.50	325.50	325.50
80	325.50	325.50	325.50	325.50	325.50	325.50	325.90	325.50	325.50	325.50
90	325.50	325.50	325.50	315.90	325.50	325.50	325.90	325.50	325.50	325.50



### 4.3 Analysis and Discussion

#### 4.3.1 Rotation Speed for Servo Motor Testing

First experiment was conducted to evaluate the speed of rotation for the servo motor ranging on the road using the road model. The aim of this experiment is to determine the suitable speed for the servo motor to rotate when ranging the road surface. The suitable speed was determined by calculate the accuracy of the road model width. As a result of experiment, the road model profile was plotted for every delay functions as shown in Graph 4.1. From the graph, the road region was started at  $34^\circ$  and finished at  $148^\circ$ .

Table 4.6 Initial angle of road region,  $\theta_i$  and final angle of road region,  $\theta_f$  for every time delay function.

Time delay function, $ms$	Initial angle of road region, $\theta_i$ ( $^\circ$ )	Final angle of road region, $\theta_f$ ( $^\circ$ )
50	35	149
40	33	151
30	31	152
20	31	150
10	32	152

The measure value road model width was calculated by using equation (25). The actual value road model width is 92 cm.

$$R = d \sin\left(\frac{\theta_f - \theta_i}{2}\right) \times 2 \quad (25)$$

Where,  $R$  is the measured value road model width,  $d$  is the distance between the sensor and the road model surface at angle  $\frac{\theta_f + \theta_i}{2}$ ,  $\theta_f$  is the final angle of the road model region and  $\theta_i$  is the initial angle of the road model region.

The Percentage of error was also calculated using formula (26) and the percentage of accuracy was also calculated using formula (27).

$$\text{Error (\%)} = \frac{\text{Actual value} - \text{Measured value}}{\text{Actual value}} \times 100\% \quad (26)$$

$$\text{Accuracy (\%)} = 1 - \left| \frac{\text{Actual value} - \text{Measured value}}{\text{Actual value}} \right| \times 100\% \quad (27)$$

Table 4.7 Percentage of error and Percentage of accuracy for every time delay function

Time delay function, <i>ms</i>	Measured value, <i>cm</i>	Actual value, <i>cm</i>	Percentage of error, %	Percentage of accuracy, %
50	98.00	92.00	6.52	93.48
40	100.00	92.00	8.70	91.30
30	101.69	92.00	10.53	89.47
20	100.67	92.00	9.42	90.58
10	100.67	92.00	9.42	90.58

From the calculation, for 50 *ms* delay the measured value is 98 *cm* and 100 *cm* for 40 *ms* delay. Meanwhile, for 30 *ms*, 20 *ms* and 10 *ms* are 101.69 *cm*, 100.67 *cm* and 100.67 *cm* respectively. The percentage of error for 50 *ms* is 6.52 %, for 40 *ms* is 8.70 % and for 30 *ms* is 10.53 %. Then, the percentage of error for 20 *ms* and 10 *ms* are equally to 9.42 % respectively. Hence, the 50 *ms* time delay is a suitable for rotation speed of servo motor to rotate when ranging the road surface. It means the servo motor will delay in 50 *ms* for every degree of rotation and it is also to ensure the sensor can receive completely the reflected wave from the road surface and produce the accurate distance between the sensor and the road surface. Besides, the percentage error is 6.52%, it is the lowest percentage among the others and it also means the accuracy of road width is the highest with 93.48 % of accuracy percentage. As a conclusion, the 50 *ms* delay function was chose to implement on the instrument.

### 4.3.2 Accuracy Testing

This experiment was performed to evaluate the accuracy of the road width measured by the instrument. The aim for this experiment to compare with the measured value and the actual value of road width by the percentage of error and the percentage of accuracy. The experiment was conducted on the road with 1 lane and road had road curb along it side. The actual width of road with 1 lane is 4.16 m and the actual width of road had road curb is 7.05 m. The table shows the 10 times of data were taken for angle rotation and the distance between the device and the surface of road. The road profiles were also plotted.

Road with 1 lane:

Table 4.8 Initial angle of road region,  $\theta_i$  and final angle of road region,  $\theta_f$  for 10 trials

No. of trials	Initial angle of road region, $\theta_i$ (°)	Final angle of road region, $\theta_f$ (°)
1	4	170
2	6	169
3	6	170
4	5	170
5	5	170
6	4	170
7	5	170
8	5	170
9	6	170
10	6	169

Road had road curb:

Table 4.9 Initial angle of road region,  $\theta_i$  and final angle of road region,  $\theta_f$  for 10 trials

No. of trials	Initial angle of road region, $\theta_i$ (°)	Final angle of road region, $\theta_f$ (°)
1	23	162
2	21	163
3	22	163
4	25	163
5	24	162
6	24	161
7	25	162
8	27	160
9	20	162
10	26	163

The measure value road model width was calculated by using equation (25). The actual value road width is 416 cm and the actual value road width for road had road curb is 705 cm.

$$R = d \sin\left(\frac{\theta_f - \theta_i}{2}\right) \times 2 \quad (25)$$

Where,  $R$  is the measured value road model width,  $d$  is the distance between the sensor and the road model surface at angle  $\frac{\theta_f + \theta_i}{2}$ ,  $\theta_f$  is the final angle of the road model region and  $\theta_i$  is the initial angle of the road model region.

The Percentage of error was also calculated using formula (26) and the percentage of accuracy was also calculated using formula (27).

$$\text{Error (\%)} = \frac{\text{Actual value} - \text{Measured value}}{\text{Actual value}} \times 100\% \quad (26)$$

$$\text{Accuracy (\%)} = 1 - \left| \frac{\text{Actual value} - \text{Measured value}}{\text{Actual value}} \right| \times 100\% \quad (27)$$



Road with 1 lane:

Table 4.10 Percentage of error and Percentage of accuracy for 10 trials

No. of trials	Measured value, cm	Actual value, cm	Percentage of error, %	Percentage of accuracy, %
1	347.91	416.00	16.37	83.63
2	346.70	416.00	16.70	83.30
3	347.12	416.00	16.56	83.44
4	347.52	416.00	16.46	83.54
5	349.50	416.00	15.98	84.02
6	347.91	416.00	16.37	83.63
7	347.52	416.00	16.46	83.54
8	349.50	416.00	15.98	84.02
9	347.12	416.00	16.56	83.44
10	346.70	416.00	16.70	83.30
Average	347.75	416.00	16.414	83.59

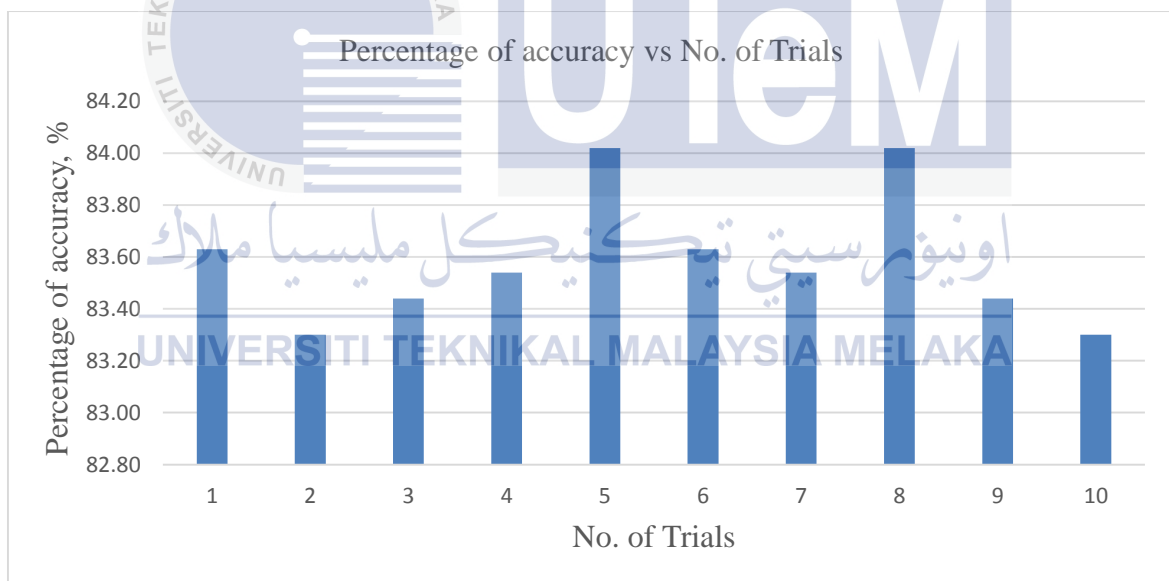


Figure 4.7 Graph of Percentage accuracy vs No. of Trials (road with 1 lane)

Figure 4.7 shows the percentage of accuracy against no. of trials for road with 1 lane. Based on the graph, the percentage accuracy of the instrument for measuring road width is in the range of 83.30% and 84.02%. The highest percentage of accuracy is 84.02%, the lowest percentage of accuracy is 83.30% and the average of percentage accuracy is 83.59%. The average percentage of accuracy of the instrument on the road with 1 lane is merely less

2.46% than average percentage of accuracy of the instrument on the road had road curb. In addition, the road surface on the road with 1 lane is rough compared to the road surface on the road had road curb thus it affect the measured value of road width to become less accurate. As a conclusion, the instrument for road width measurement is accurate as the percentage of accuracy is more than 50%.

Road had road curb:

Table 4.11 Percentage of error and Percentage of accuracy for 10 trials

No. of trials	Measured value, <i>cm</i>	Actual value, <i>cm</i>	Percentage of error, %	Percentage of accuracy, %
1	609.77	705.00	13.51	86.49
2	597.38	705.00	15.27	84.73
3	613.66	705.00	12.96	87.04
4	608.51	705.00	13.69	86.31
5	607.76	705.00	13.79	86.21
6	605.70	705.00	14.08	85.92
7	605.70	705.00	14.08	85.92
8	597.01	705.00	15.32	84.68
9	615.53	705.00	12.69	87.31
10	605.70	705.00	14.08	85.92
Average	606.67	705.00	13.95	86.05

UNIVERSITI TEKNIKAL MALAYSIA MELAKA

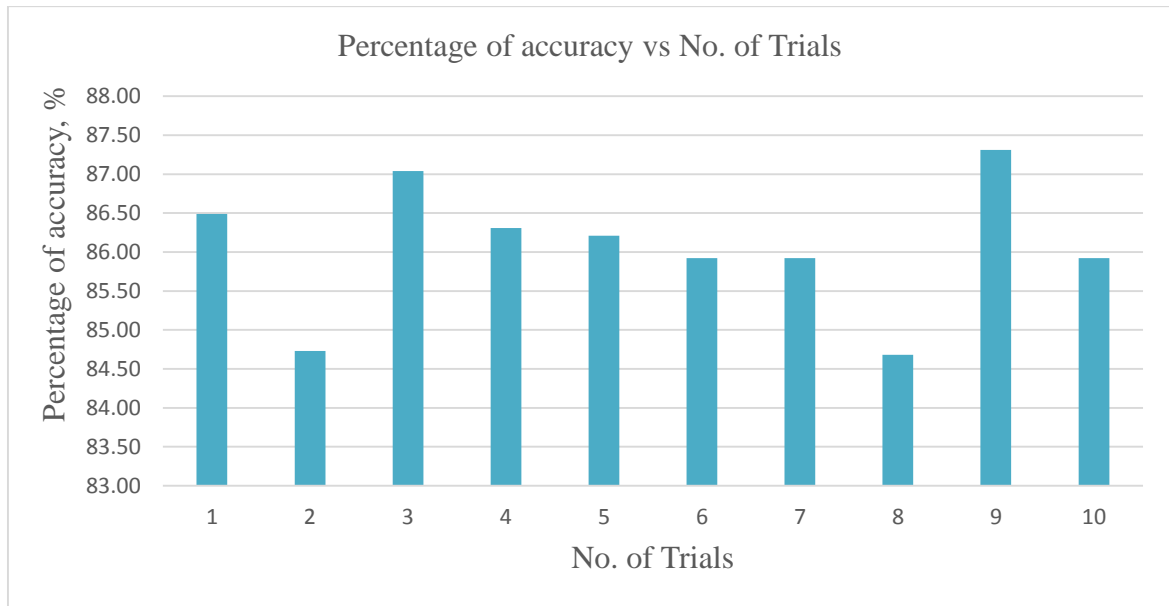


Figure 4.8 Graph of Percentage accuracy vs No. of Trials (road had road curb)

Figure 4.8 shows the percentage of accuracy against no. of trials for road had road curb. Based on the graph, the percentage accuracy of the instrument for measuring road width is in the range of 84.68% and 87.31%. The highest percentage of accuracy is 87.31%, the lowest percentage of accuracy is 84.68% and the average of percentage accuracy is 86.05%. There are a slightly 2.46% more accurate in term of accuracy for measure the road width for road had road curb compared to for measure the road width for road width 1 lane. It is because the road surface for road had road curb is smoother than the road surface for road with 1 lane. In short, the percentage of accuracy of the instrument to measure road width is more than 50% hence the instrument is accurate to measure the road width.

### 4.3.3 Reliability Testing

In this reliability testing, 30 data were collected from the output of the ultrasonic sensor when ranging on the road with 1 lane and the road had road curb along it side. From the data collected, the road profile was plotted and determine the road region from the graph. The initial angle and final angle of road region was also determined as shown below.

Road with 1 lane:

4.12 Initial angle of road region,  $\theta_i$  and final angle of road region,  $\theta_f$  for 30 trials

No. of trials	Initial angle of road region, $\theta_i$ (°)	Final angle of road region, $\theta_f$ (°)
1	4	170
2	6	169
3	6	170
4	5	170
5	5	170
6	4	170
7	5	170
8	5	170
9	6	170
10	6	169
11	4	170
12	6	169
13	6	170
14	5	170
15	5	170
16	4	170
17	5	170
18	5	170
19	6	170
20	6	169
21	4	170

22	6	169
23	6	170
24	5	170
25	5	170
26	4	170
27	5	170
28	5	170
29	6	170
30	6	169

Road had road curb:

4.13 Initial angle of road region,  $\theta_i$  and final angle of road region,  $\theta_f$  for 30 trials

No. of trials	Initial angle of road region, $\theta_i$ (°)	Final angle of road region, $\theta_f$ (°)
1	23	162
2	21	163
3	22	163
4	25	163
5	24	162
6	24	161
7	25	162
8	27	160
9	20	162
10	26	163
11	26	163
12	27	160
13	20	162
14	25	162
15	24	162
16	24	161
17	25	163
18	21	163
19	22	163

20	23	162
21	23	162
22	22	163
23	24	162
24	25	162
25	20	162
26	26	163
27	27	160
28	24	161
29	25	163
30	21	163

The measure value road model width was calculated by using equation (25). The actual value road width is 416 cm and the actual value road width for road had road curb is 705 cm.

$$R = d \sin\left(\frac{\theta_f - \theta_i}{2}\right) \times 2 \quad (25)$$

Where,  $R$  is the measured value road model width,  $d$  is the distance between the sensor and the road model surface at angle  $\frac{\theta_f + \theta_i}{2}$ ,  $\theta_f$  is the final angle of the road model region and  $\theta_i$  is the initial angle of the road model region.

The Percentage of error was also calculated using formula (26) and the percentage of accuracy was also calculated using formula (27).

$$\text{Error (\%)} = \frac{\text{Actual value} - \text{Measured value}}{\text{Actual value}} \times 100\% \quad (26)$$

$$\text{Accuracy (\%)} = 1 - \left| \frac{\text{Actual value} - \text{Measured value}}{\text{Actual value}} \right| \times 100\% \quad (27)$$

$$\text{Precision} = 1 - \left| \frac{X_n - \bar{X}_n}{\bar{X}_n} \right| \quad (28)$$

Where  $X_n$  is the value of  $n^{th}$  measurement and  $\bar{X}_n$  is average of measurement

Road with 1 lane:

Table 4.14 Percentage of error, Percentage of accuracy and Precision value for 30 trials

No. of trials	Measured value, cm	Actual value, cm	Percentage of error, %	Percentage of accuracy, %	Precision value
1	347.91	416.00	16.37	83.63	0.9995
2	346.70	416.00	16.70	83.30	0.9970
3	347.12	416.00	16.56	83.44	0.9982
4	347.52	416.00	16.46	83.54	0.9993
5	349.50	416.00	15.98	84.02	0.9950
6	347.91	416.00	16.37	83.63	0.9995
7	347.52	416.00	16.46	83.54	0.9993
8	349.50	416.00	15.98	84.02	0.9950
9	347.12	416.00	16.56	83.44	0.9982
10	346.70	416.00	16.70	83.30	0.9970
11	347.91	416.00	16.37	83.63	0.9995
12	346.70	416.00	16.70	83.30	0.9970
13	347.12	416.00	16.56	83.44	0.9982
14	347.52	416.00	16.46	83.54	0.9993
15	349.50	416.00	15.98	84.02	0.9950
16	347.91	416.00	16.37	83.63	0.9995
17	347.52	416.00	16.46	83.54	0.9993
18	349.50	416.00	15.98	84.02	0.9950
19	347.12	416.00	16.56	83.44	0.9982
20	346.70	416.00	16.70	83.30	0.9970
21	347.91	416.00	16.37	83.63	0.9995
22	346.70	416.00	16.70	83.30	0.9970
23	347.12	416.00	16.56	83.44	0.9982
24	347.52	416.00	16.46	83.54	0.9993
25	349.50	416.00	15.98	84.02	0.9950
26	347.91	416.00	16.37	83.63	0.9995
27	347.52	416.00	16.46	83.54	0.9993
28	349.50	416.00	15.98	84.02	0.9950
29	347.12	416.00	16.56	83.44	0.9982
30	346.70	416.00	16.70	83.30	0.9970
Average	347.75	416.00	16.41	83.59	0.9978

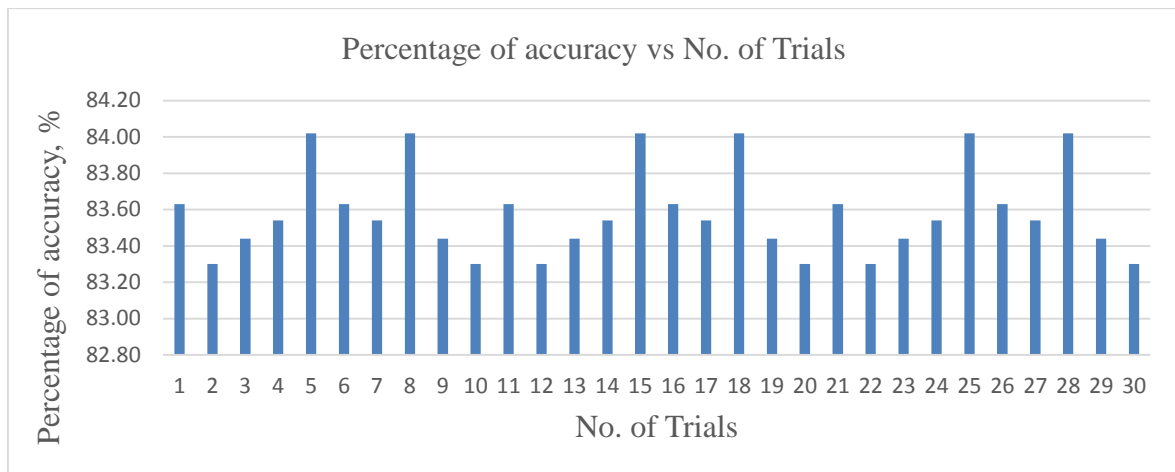


Figure 4.9 Graph of Percentage accuracy vs No. of Trials (road with 1 lane)

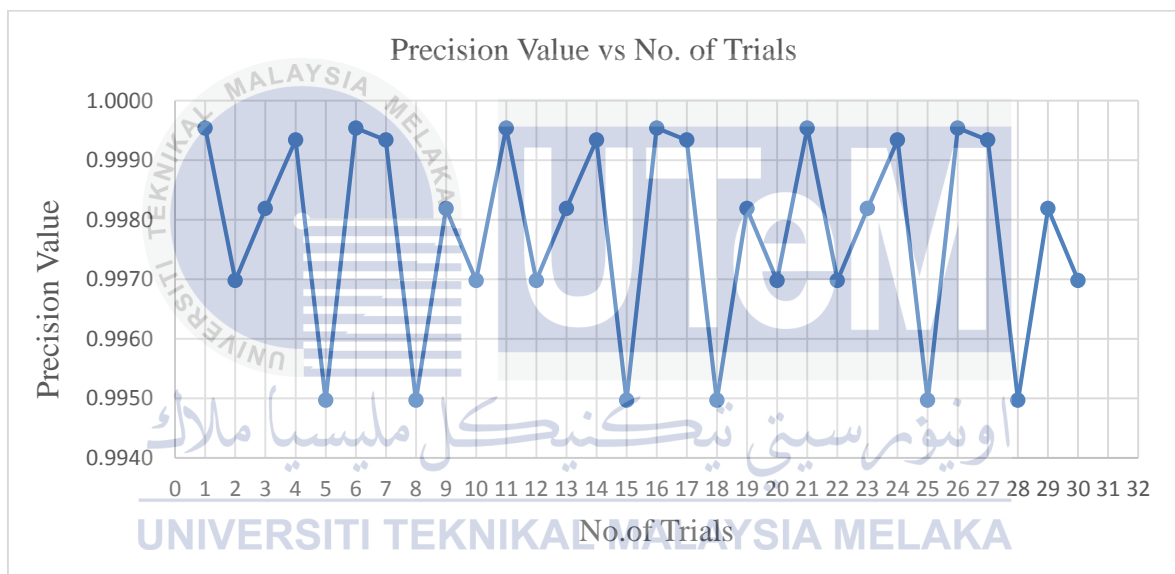


Figure 4.10 Graph of Precision value vs No. of Trials (road with 1 lane)

Figure 4.9 shows the percentage accuracy against no. of trials for road with 1 lane for reliability experiment. The data were collected for 30 times to determine the reliability of the instrument for measuring the road width. From the graph, the percentage of accuracy is in the range of 83.30% and 84.02%, the highest percentage of accuracy is 84.02% and the lowest percentage of accuracy is 83.30%. The average of 30 data percentage of accuracy is 83.59%. The average value of precision value for the measurement is 0.99. As a conclusion, the collected data is show that the data is repeatable and reliable on measure the road width of the road with 1 lane.



Road had road curb:

Table 4.15 Percentage of error, Percentage of accuracy and Precision value for 30 trials

No. of trials	Measured value, cm	Actual value, cm	Percentage of error, %	Percentage of accuracy, %	Precision value
1	609.77	705.00	13.51	86.49	0.9949
2	597.38	705.00	15.27	84.73	0.9847
3	613.66	705.00	12.96	87.04	0.9885
4	608.51	705.00	13.69	86.31	0.9970
5	607.76	705.00	13.79	86.21	0.9982
6	605.70	705.00	14.08	85.92	0.9984
7	605.70	705.00	14.08	85.92	0.9984
8	597.01	705.00	15.32	84.68	0.9841
9	615.53	705.00	12.69	87.31	0.9854
10	605.70	705.00	14.08	85.92	0.9984
11	605.70	705.00	14.08	85.92	0.9984
12	597.01	705.00	15.32	84.68	0.9841
13	615.53	705.00	12.69	87.31	0.9854
14	605.70	705.00	14.08	85.92	0.9984
15	607.76	705.00	13.79	86.21	0.9982
16	605.70	705.00	14.08	85.92	0.9984
17	608.51	705.00	13.69	86.31	0.9970
18	597.38	705.00	15.27	84.73	0.9847
19	613.66	705.00	12.96	87.04	0.9885
20	609.77	705.00	13.51	86.49	0.9949
21	609.77	705.00	13.51	86.49	0.9949
22	613.66	705.00	12.96	87.04	0.9885
23	607.76	705.00	13.79	86.21	0.9982
24	605.70	705.00	14.08	85.92	0.9984
25	615.53	705.00	12.69	87.31	0.9854
26	605.70	705.00	14.08	85.92	0.9984
27	597.01	705.00	15.32	84.68	0.9841
28	605.70	705.00	14.08	85.92	0.9984
29	608.51	705.00	13.69	86.31	0.9970
30	597.38	705.00	15.27	84.73	0.9847
Average	606.67	705.00	13.95	86.05	0.9928

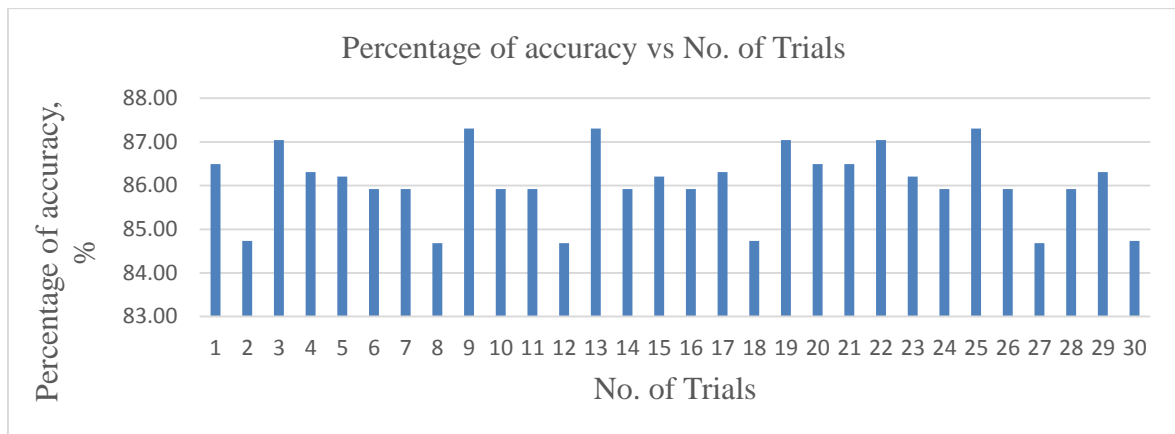


Figure 4.11 Graph of Percentage accuracy vs No. of Trials (road had road curb)

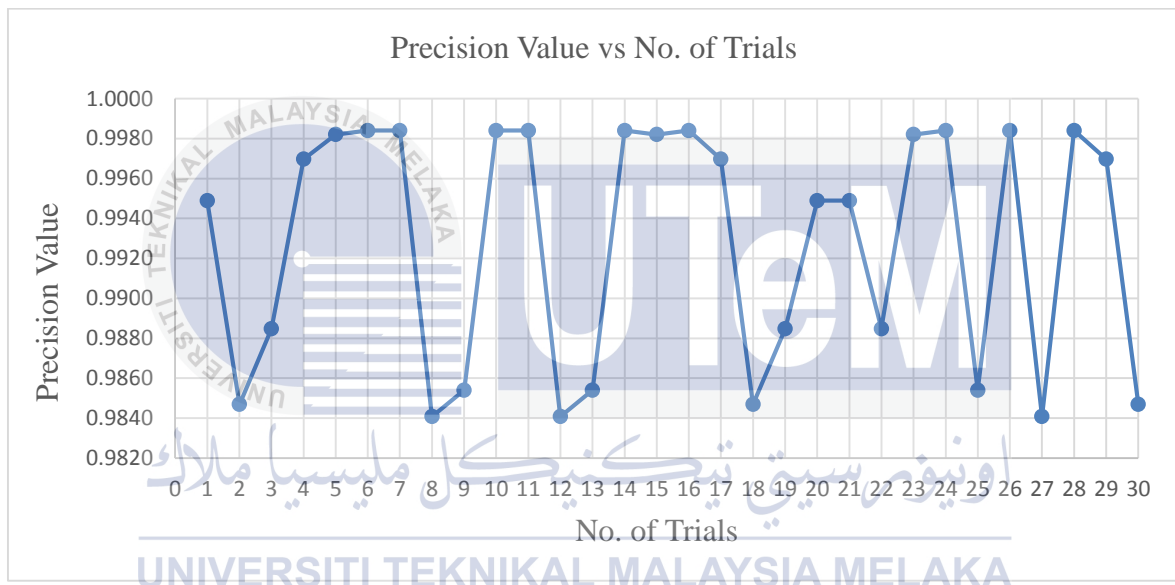


Figure 4.12 Graph of Precision value vs No. of Trials (road had road curb)

Figure 4.11 shows the percentage accuracy against no. of trials for road had road curb along it side for reliability experiment. The data were collected for 30 times to determine the reliability of the instrument for measuring the road width. From the graph, the percentage of accuracy is in the range of 84.68% and 87.31%, the highest percentage of accuracy is 87.31% and the lowest percentage of accuracy is 84.68%. The average of 30 data percentage of accuracy is 86.05%. The average value of precision value for the measurement is 0.99, same as the measurement for road with 1 lane. As a conclusion, the collected data is show that the data is repeatable and reliable on measure the road width of the road had road curb.

## CHAPTER 5

### CONCLUSION AND RECOMMENDATIONS

This chapter will conclude all the experiment's result obtained. Besides, some problem that overwhelm while working on this project also discussed.

#### 5.1 Conclusion

Road line is one of the properties on the road and it is important to give a guidance for the road user like car driver and motorist. Road line painting will provide a guidance to vehicle's user while driving on the road. As a conclusion, this sensor development was important for road line painting industry in Malaysia. The sensor was designed and developed in this final year project to measure the road width. The sensor can measure the road width for road with lane and road had road curb along its side after the experiment was done. As a result, the first objective to design and develop an instrument to measure road width was achieved. The design of sensor's accuracy and reliability was developed in order to achieve the second objective for this project. As a result, the percentage of accuracy to measure the road with 1 lane is 83.59% and the percentage of accuracy to measure the road had road curb is 86.05%. Therefore, the instrument is accurate to measure the road width for road line painting industry. In terms of reliability, the measured value from the instrument shows the instrument is able to produce repeatability measured value for road width measurement with 0.99% of precision value.

During PSM, it needs the fundamental knowledge in handling the project. The ability to gain information from many source such as internet information, reference book, product datasheet, journal that related with this project and discussion with the supervisor are a crucial task. Then, all information need to be analysed and sorted it according the related part. SolidWorks software used to design the hardware section for this sensor. In PSM, the process designed was accomplished and hardware fabrication and data analysed were done in PSM2.

## 5.2 Recommendation

In this project, some weakness that can be made later in the future. The enhancement that can be done is to find how to measure the road width on the road surface is rough. In this project, there are a problem that overwhelm while working to measure on the rough road surface. In addition, this instrument system mode also can be improved by done it in autonomous mode. Recently, the road region is determine manually from the graph so to make it more flexible is must be done automatically in detection of road region. Besides, the improvement will be further explored in the research on multi-sensor so that the sensor for road and road-edge detection can better adapt to the road environment.

. In PSM, a lot of information are collected from all the sources. It will be easy to analyse the information if it sorted according to their characteristic that related to the project.

## REFERENCES

- [1] Yaacob, N.F, Pekerja Cat Jalan Dirempuh, Sinar Harian, December 2013
- [2] Handbook of Modern Sensors Physics, Design and Applications, 4<sup>th</sup>. ed., Springer Science+Business Media, LLC, 223 Spring Street, New York, NY, 2010.
- [3] Handbook of Sensors and Transducers, 1<sup>st</sup> ed., Auris Reference Ltd., UK, 2012.
- [4] Sahri, Mohd Shahrizan (2007) A study of ultrasonic car braking system. Undergraduates Project Report (PSM) thesis, Universiti Malaysia Pahang.
- [5] S. Kodagoda, E. A. S. M. Hemachandra, P. G. Jayasekara, R. L. Peiris, and A. C. De Silva, "Obstacle Detection and Map Building with a Rotating Ultrasonic Range Sensor using Bayesian Combination," vol. 00, 2006.
- [6] C. Wolff, Radar Tutorial [online]. Available at: <http://www.radartutorial.eu/01.basics/rb02.en.html>
- [7] RADAR (Radio Detection and Ranging) [online]. Available at: <http://www.engineersgarage.com/articles/what-is-radar-technology?page=1>
- [8] Z. Hu, H. Wang, L. Zhang, and H. Yu, "Laser sensor based road boundary recognition of mobile robot," *2009 Int. Conf. Networking, Sens. Control*, pp. 210–215, Mar. 2009.
- [9] W. Zhang, "LIDAR-based road and road-edge detection," *2010 IEEE Intell. Veh. Symp.*, pp. 845–848, Jun. 2010.
- [10] LiDAR UK [online]. Available at: <http://www.lidar-uk.com/>
- [11] M. Feng, P. Jia, X. Wang, H. Liu, and J. Cao, "Structural Road Detection for Intelligent Vehicle Based on a 2d Laser Radar," *2012 4th Int. Conf. Intell. Human-Machine Syst. Cybern.*, pp. 293–296, Aug. 2012.
- [12] R. Liu, "A 3-D Real-Time Road Edge Detection System for Automated Smart Car Control," *2006 IEEE Int. Conf. Networking, Sens. Control*, pp. 837–841, 2006.
- [13] W. Wu and G. ShuFeng, "Research on Unstructured Road Detection Algorithm Based on the Machine Vision," *2009 Asia-Pacific Conf. Inf. Process.*, pp. 112–115, Jul. 2009.
- [14] Cytron Technologies High Resolution Ultrasonic Range Finder. MaxBotix SN-LV-EZ1 Datasheet. 2012

[15] Cytron Tecnologies RC Servo Motor. C36R User Manual. April 2013



NO	ACTIVITIES	SCHEDULE 2014														
		WEEK 1	WEEK 2	WEEK 3	WEEK 4	WEEK 5	WEEK 6	WEEK 7	WEEK 8	WEEK 9	WEEK 10	WEEK 11	WEEK 12	WEEK 13	WEEK 14	WEEK 15
1	START DESIGN HARDWARE															
2	RECEIVED APPROVAL HARDWARE DESIGN															
3	PLANNING MATERIALS TO DEVELOP SENSOR															
4	DEVELOP SENSOR															
5	SOFTWARE PREPARATION FOR EXPERIMENT															
6	SOFTWARE DEVELOPMENT EXPERIMENT															
7	DRAFTING CHAPTER 1(REPORT)															
8	ANALYSING DATA AND DEVELOP SOFTWARE															
9	DRAFTING CHAPTER 2(REPORT)															
10	PERFORMANCE EXPERIMENT															
11	DRAFTING CHAPTER 3(REPORT)															
12	ANALYSING DATA FOR PERFORMANCE EXPERIMENT															
13	DRAFTING CHAPTER 4(REPORT)															
14	DRAFTING CHAPTER 5(REPORT)															
15	COMPLETING REPORT PSM 2															
16	SUBMIT PSM FULL REPORT TO THE SUPERVISOR AND PANEL															
17	PRESENTATION															

PSM Gantt Chart

## APPENDIX 1





## APPENDIX 3

## Sensor Design

